

$a_0(980)$ -meson twist-2 distribution amplitude within the QCD sum rules and investigation of $D \rightarrow a_0(980)(\rightarrow \eta\pi)e^+\nu_e$

Zai-Hui Wu, Hai-Bing Fu,^{*} Tao Zhong,[†] and Dong Huang
Department of Physics, Guizhou Minzu University, Guiyang 550025, China

Dan-Dan Hu and Xing-Gang Wu[‡]
*Department of Physics, Chongqing Key Laboratory for Strongly Coupled Physics,
 Chongqing University, Chongqing 401331, China*
 (Dated: November 11, 2022)

In this paper, the moments of $a_0(980)$ -meson twist-2 light-cone distribution amplitudes were deeply researched by using the QCD sum rules approach within the background field theory. Up to 9_{th}-order accuracy, we present $\langle \xi_{2;a_0}^n \rangle|_{\mu_0}$ at the initial scale $\mu_0 = 1$ GeV, i.e. $\langle \xi_{2;a_0}^1 \rangle|_{\mu_0} = -0.307(43)$, $\langle \xi_{2;a_0}^3 \rangle|_{\mu_0} = -0.181(34)$, $\langle \xi_{2;a_0}^5 \rangle|_{\mu_0} = -0.078(28)$, $\langle \xi_{2;a_0}^7 \rangle|_{\mu_0} = -0.049(26)$, $\langle \xi_{2;a_0}^9 \rangle|_{\mu_0} = -0.036(24)$, respectively. An improved light-cone harmonic oscillator model is then adopted for the $a_0(980)$ -meson twist-2 light-cone distribution amplitudes, whose input parameters are then fixed by using the least squares method based on the $\langle \xi_{2;a_0}^n \rangle|_{\mu_0}$, and their goodness of fit can reach to 93%. Then, we calculate the $D \rightarrow a_0(980)$ transition form factors within the light-cone sum rules approach, and at largest recoil point, we obtain $f_+^{D \rightarrow a_0}(0) = 1.058_{-0.035}^{+0.068}$ and $f_-^{D \rightarrow a_0}(0) = 0.764_{-0.036}^{+0.044}$. As a further application, the branching fractions of the $D \rightarrow a_0(980)\ell\bar{\nu}_\ell$ semileptonic decays are given. Taking the decay $a_0(980) \rightarrow \eta\pi$ into consideration, we obtain $\mathcal{B}(D^0 \rightarrow a_0(980)^-(\rightarrow \eta\pi^-)e^+\nu_e) = (1.292_{-0.092}^{+0.194}) \times 10^{-4}$, $\mathcal{B}(D^+ \rightarrow a_0(980)^0(\rightarrow \eta\pi^0)e^+\nu_e) = (1.628_{-0.116}^{+0.244}) \times 10^{-4}$, which are consistent with the BESIII collaboration and PDG data within errors.

PACS numbers: 12.38.-t, 12.38.Bx, 14.40.Aq

I. INTRODUCTION

In the past few decades, especially for the discovery of the resonance $a_0(980)$ [1], the properties of scalar mesons still remain the controversial, which become hot topics in hadron physics. Theoretically, they have been considered as tetraquark states [2–6] or two-meson bound states [7–11]. In the literature, $a_0(980)$ is usually taken as a scalar meson with $q\bar{q}$ configuration based on the constituent quark model. In the present paper, we shall adopt this $q\bar{q}$ configuration for $a_0(980)$ and make a detailed study on its twist-2 light-cone distribution amplitudes, which can be tested when more accurate data have been achieved in the near future.

The semileptonic decay of the charmed meson provides simpler decay mechanism and final-state interactions, and it is an ideal platform for studying the meson's properties. The BESIII collaboration observed the charmless hadronic decay processes involving $a_0(980)$ -meson, and reported the results of $D^0 \rightarrow a_0(980)^-e^+\nu_e$ and $D^+ \rightarrow a_0(980)^0e^+\nu_e$ with the significance up to 6.4σ and 2.9σ , respectively [12]. The branching ratio of $D \rightarrow a_0(980)\ell\bar{\nu}_\ell$ combining with $a_0(980)$ -meson decays $a_0(980) \rightarrow \eta\pi$ are $\mathcal{B}(D^0 \rightarrow a_0(980)^-e^+\nu_e) \times \mathcal{B}(a_0(980)^- \rightarrow \eta\pi^-) =$

$(1.33_{-0.29}^{+0.33} \pm 0.09) \times 10^{-4}$ and $\mathcal{B}(D^+ \rightarrow a_0(980)^0e^+\nu_e) \times \mathcal{B}(a_0(980)^0 \rightarrow \eta\pi^0) = (1.66_{-0.66}^{+0.81} \pm 0.11) \times 10^{-4}$, where the first and second errors are statistical error and systematic error, respectively. Recently, the BESIII collaboration presented the branching ratio of the decay $D_s^+ \rightarrow f_0(980)(\rightarrow \pi^0\pi^0)e^+\nu_e$ for the first time [13], by using the 6.32 fb^{-1} e^+e^- collision data recorded with the center-of-mass energies between 4.178 GeV to 4.226 GeV. These experimental values will help us to study the production mechanism of scalar mesons through the hadron decay process. The $D \rightarrow a_0(980)\ell\bar{\nu}_\ell$ semileptonic decays also provide ideal platforms for deep learning of the $a_0(980)$ -meson and its related preferences. And the important parameters for the semileptonic decays $D \rightarrow a_0(980)\ell\bar{\nu}_\ell$, many theoretical methods have been employed to calculate the transition form factors (TFFs), such as the covariant confined quark model (CCQM) [14], the light-cone sum rules (LCSR) [15, 16] and the anti-de Sitter with QCD potential AdS/QCD [17].

The LCSR is an effective method in dealing with the heavy to light decays. It applies a partial resummation of the operator product expansion to all orders and reorganizes the operator production expansion in terms of the twists of relevant operators, which then results in a series over the light-meson's light-cone distribution amplitudes (LCDAs) of increasing twists. The LCSR is applicable in a wide q^2 -region and could be extended to all q^2 -regions via proper extrapolations. In this paper, we will adopt the LCSR to calculate the $D \rightarrow a_0(980)$ TFFs. One of the key quantities that characterize the TFFs is the

^{*}Electronic address: fuhb@cqu.edu.cn (corresponding author)

[†]Electronic address: zhongtao1219@sina.com

[‡]Electronic address: wuxg@cqu.edu.cn

twist-2 LCDA, which describes the dominant momentum fraction distribution for each part of a meson. In general, the $a_0(980)$ -meson twist-2 LCDA $\phi_{2;a_0}(x, \mu)$ can be expanded as a Gegenbauer polynomial series [18]

$$\phi_{2;a_0}(x, \mu) = 6x\bar{x} \left[a_{2;a_0}^0(\mu) + \sum_{n=1}^{\infty} a_{2;a_0}^n(\mu) C_n^{3/2}(\xi) \right], \quad (1)$$

where $\bar{x} = (1 - x)$ and $\xi = (2x - 1)$. The even Gegenbauer coefficients are highly suppressed, which exactly equal to zero under the approximation that $m_1 \simeq m_2$ ($m_{1,2}$ are masses of two constituent quarks), and the LCDA of the scalar meson is then dominated by the odd Gegenbauer moments. In contrast, the odd Gegenbauer moments vanish for π and ρ mesons. Thus, it tends to the antisymmetric form under $u \rightarrow (1 - u)$ transition in the $SU_f(3)$ limit. Currently, the $a_0(980)$ -meson twist-2 LCDA is mainly coming from QCDSR by Cheng, Chua and Yang [18], which gives the first two order Gegenbauer moments. To have a deeper insight into the $a_0(980)$ -meson twist-2 LCDA and to improve the accuracy of the processes involving $a_0(980)$ -meson, it is helpful to know its higher order Gegenbauer moments, which can be achieved by establishing a light-cone harmonic oscillator (LCHO) model with the help of the Brodsky-Huang-Lepage (BHL) prescription. The LCHO model parameters can be fixed by fitting them to the known moments $\langle \xi_{2;a_0}^n \rangle|_{\mu}$ at a specified scale μ with the least squares method.

For the purpose, we need to calculate the $a_0(980)$ -meson twist-2 LCDA moments $\langle \xi_{2;a_0}^n \rangle|_{\mu}$. As one of the effective way to calculate each order moments for light or heavy meson twist-2 or twist-3 LCDA is the QCDSR under the framework of the background field theory (BFTSR). The basic assumption of QCDSR is the introduction of vacuum condensates. In addition, QCD background field method systematically describes these vacuum condensates from the perspective of field theory [19–28]. Quark and gluon fields are composed of background fields and quantum fluctuations around them under the framework of BFTSR. The vacuum condensates and quantum fluctuations of the background field represent non perturbative effects and computable perturbative effects respectively. These vacuum condensates provide a clear physical image for the internal structure of the bound state, which makes the calculation easier. At present, the BFTSR has been applied to calculate the LCDAs of pseudoscalar and vector/axial vector mesons [29–37]. In this paper, we will study the scalar $a_0(980)$ -meson twist-2 LCDA by using BFTSR firstly.

The remaining parts of this paper are organized as follows. In Sec. II, we calculate the $a_0(980)$ -meson twist-2 LCDA moments and introduce the LCHO model. A new improved model is proposed and the model parameters shall be obtained by fitting moment with the least square method. Section III gives the numerical results and discussions. Section IV is for a brief summary.

II. THEORETICAL FRAMEWORK

The $a_0(980)$ -meson have three types of states, one is $a_0(980)^0$ -meson with $(\bar{u}u - \bar{d}d)/\sqrt{2}$ component, the other is $a_0(980)^-$ -meson with $(\bar{u}d)$ component, and the third one is $a_0(980)^+$ -meson with $(\bar{d}u)$. Based on the basic procedure of QCD sum rules, one can adopt the following two-point correlator to derive the sum rules for $a_0(980)$ -meson twist-2 LCDA moments $\langle \xi_{2;a_0}^n \rangle|_{\mu}$, which can be read off,

$$\begin{aligned} \Pi_{2;a_0}^{(n,0)}(z, q) &= i \int d^4x e^{iq \cdot x} \langle 0 | T \{ J_n^V(x), J_0^{S,\dagger}(0) \} | 0 \rangle \\ &= (z \cdot p)^{n+1} I_{2;a_0}^{(n,0)}(q^2), \end{aligned} \quad (2)$$

where $z^2 = 0$ and n take odd numbers. The currents are taken as $J_n^V(x) = \bar{q}_1(x) \not{x} (iz \cdot \vec{D})^n q_2(x)$ and $J_0^S(0) = \bar{q}_1(0) q_2(0)$ with the covariant derivative $(iz \cdot \vec{D})^n = (iz \cdot \vec{D} - iz \cdot \vec{D})^n$, which are mainly come from definitions of the scalar $a_0(980)$ -meson twist-2 LCDA $\phi_{2;a_0}(x, \mu)$ and twist-3 LCDA $\phi_{3;a_0}^p(x, \mu)$, which can be written as [18]

$$\begin{aligned} \langle 0 | \bar{q}_1(z) \gamma_\mu q_2(-z) | a_0(p) \rangle \\ = p_\mu f_{a_0} \int_0^1 dx e^{i(2u-1)(p \cdot z)} \phi_{2;a_0}(x, \mu), \end{aligned} \quad (3)$$

$$\begin{aligned} \langle 0 | \bar{q}_1(z) q_2(-z) | a_0(p) \rangle \\ = m_{a_0} f_{a_0} \int_0^1 dx e^{i(2u-1)(p \cdot z)} \phi_{3;a_0}^p(x, \mu), \end{aligned} \quad (4)$$

From one side, one can apply the OPE for the correlator, e.g. Eq. (2) in deep Euclidean region $q^2 \ll 0$. Then, the correlator can be expanded into three terms including the quark propagators and the vertex operators,

$$\begin{aligned} \Pi_{2;a_0}^{(n,0)}(z, q) &= i \int d^4x e^{iq \cdot x} \left\{ \right. \\ &\quad - \text{Tr} \langle 0 | S_F^{q_1}(0, x) \not{x} (iz \cdot \vec{D})^n S_F^{q_2}(x, 0) | 0 \rangle \\ &\quad + \text{Tr} \langle 0 | \bar{q}_1(x) q_1(0) \not{x} (iz \cdot \vec{D})^n S_F^{q_2}(x, 0) | 0 \rangle \\ &\quad + \text{Tr} \langle 0 | S_F^{q_1}(0, x) \not{x} (iz \cdot \vec{D})^n \bar{q}_2(x) q_2(0) | 0 \rangle \\ &\quad \left. + \dots \right\} \end{aligned} \quad (5)$$

In dealing with Lorentz invariant scalar function $\Pi_{2;a_0}^{(n,0)}(z, q^2)$, the vacuum matrix element should be used, which can be found in our previous work [32]. Meanwhile, we take $q_1 = q_2 = q$ stand for the light u, d -quark. On the other hand, one can insert a complete set of $a_0(980)$ -meson intermediated hadronic states with the same J^P quantum number into the correlator and obtain the hadronic expression

$$\begin{aligned} \text{Im} I_{2;a_0, \text{had}}^{(n,0)}(q^2) &= \pi \delta(q^2 - m_{a_0}^2) f_{a_0}^2 \langle \xi_{2;a_0}^n \rangle|_{\mu} \langle \xi_{3;a_0}^{p,0} \rangle|_{\mu} \\ &\quad + \frac{3m_q}{4\pi^2(n+2)} \theta(q^2 - s_{a_0}). \end{aligned} \quad (6)$$

In which the definitions of moments for $a_0(980)$ -meson twist-2, 3 LCDAs are used, which have the following formula

$$\langle 0 | \bar{q}_1(0) \not{z} (i \vec{z} \cdot \vec{D})^n q_2(0) | a_0(p) \rangle = (z \cdot p)^{n+1} f_{a_0} \langle \xi_{2;a_0}^n \rangle |_\mu, \quad (7)$$

$$\langle 0 | \bar{q}_1(0) q_2(0) | a_0(p) \rangle = m_{a_0} f_{a_0} \langle \xi_{3;a_0}^{p;0} \rangle |_\mu. \quad (8)$$

where $m_q = m_{q_1} = m_{q_2}$ in Eqs. (6)-(8) stand for the mass of light quark and the m_{a_0} is the mass of $a_0(980)$ -meson, f_{a_0} is the decay constant. The slight difference between mass of u -quark and d -quark is ignored in this paper. Meanwhile, the s_{a_0} stands for the continuum threshold. After matching the hadronic and OPE sides through the dispersion relation and performing the Borel transformation, one can get the sum rule for $\langle \xi_{2;a_0}^n \rangle |_\mu \langle \xi_{3;a_0}^{p;0} \rangle |_\mu$,

$$\langle \xi_{2;a_0}^n \rangle |_\mu \langle \xi_{3;a_0}^{p;0} \rangle |_\mu = I_1^{\text{pert.}}(n, s_0, M^2)$$

$$\begin{aligned} & + \langle \bar{q}q \rangle I_1^{\langle \bar{q}q \rangle}(n, M^2) \\ & + \langle g_s \bar{q}q \rangle^2 I_1^{\langle g_s \bar{q}q \rangle^2}(n, M^2) \\ & + \langle g_s^2 \bar{q}q \rangle^2 I_1^{\langle g_s^2 \bar{q}q \rangle^2}(n, M^2, \mu) \\ & + \langle \alpha_s G^2 \rangle I_1^{\langle \alpha_s G^2 \rangle}(n, M^2, \mu) \\ & + \langle g_s^3 f G^3 \rangle I_1^{\langle g_s^3 f G^3 \rangle}(n, M^2, \mu) \\ & + \langle g_s \bar{q} \sigma T G q \rangle I_1^{\langle g_s \bar{q} \sigma T G q \rangle}(n, M^2). \end{aligned} \quad (9)$$

In which, we separate the sum rules into seven different terms. The detailed expressions for $I_1^i(n, s_0, M^2, \mu)$ with $i = (\text{pert.}, \langle \bar{q}q \rangle, \langle g_s \bar{q}q \rangle^2, \langle \alpha_s G^2 \rangle, \langle g_s^3 f G^3 \rangle, \langle g_s \bar{q} \sigma T G q \rangle)$ accompany by the six different vacuum condensates and perturbative terms are read off:

$$I_1^{\text{pert.}}(n, M^2) = \frac{m_q}{m_{a_0} f_{a_0}^2} e^{m_{a_0}^2/M^2} \frac{3}{8\pi^2(n+2)} \left(1 - e^{-s_0/M^2}\right), \quad (10)$$

$$I_1^{\langle \bar{q}q \rangle}(n, M^2) = \frac{2}{m_{a_0} f_{a_0}^2} e^{m_{a_0}^2/M^2}, \quad (11)$$

$$I_1^{\langle g_s \bar{q}q \rangle^2}(n, M^2) = \frac{m_q}{m_{a_0} f_{a_0}^2} e^{m_{a_0}^2/M^2} \frac{4(n+3)}{81M^4}, \quad (12)$$

$$\begin{aligned} I_1^{\langle g_s^2 \bar{q}q \rangle^2}(n, M^2, \mu) = & -\frac{2m_q}{m_{a_0} f_{a_0}^2} e^{m_{a_0}^2/M^2} \frac{2+\kappa^2}{3888\pi^2 M^4} \left\{ \delta^{0n} \left[-24 \left(-\ln \frac{M^2}{\mu^2} \right) - 148 \right] + \delta^{1n} \left[128 \left(-\ln \frac{M^2}{\mu^2} \right) - 692 \right] \right. \\ & + \theta(n-1) \left[8(6n^2+34n) \left(-\ln \frac{M^2}{\mu^2} \right) + 4n\tilde{\psi}(n) - 2(6n^2+96n+212) \right] + \theta(n-2) \left[8(33n^2-17n) \left(-\ln \frac{M^2}{\mu^2} \right) \right. \\ & - 2(6n^2+71n)\tilde{\psi}(n) - \frac{1}{n(n-1)}(231n^4+520n^3-1101n^2+230n) \left. \right] + \theta(n-3) \left[(74n-144n^2)\tilde{\psi}(n) - \frac{1}{n-1} \right. \\ & \left. \left. \times (169n^3-348n^2+245n+60) \right] + 4(n+5) \right\}, \end{aligned} \quad (13)$$

$$\begin{aligned} I_1^{\langle \alpha_s G^2 \rangle}(n, M^2, \mu) = & -\frac{2m_q}{m_{a_0} f_{a_0}^2} e^{m_{a_0}^2/M^2} \frac{1}{48\pi M^2} \left\{ 12n \left(-\ln \frac{M^2}{\mu^2} \right) - 6(n+2) + \theta(n-1) \left[4n \left(-\ln \frac{M^2}{\mu^2} \right) + 3\tilde{\psi}(n) - \frac{6}{n} \right] \right. \\ & \left. + \theta(n-2) \left[-(8n+3)\tilde{\psi}(n) - 2(2n+1) + \frac{6}{n} \right] \right\}, \end{aligned} \quad (14)$$

$$\begin{aligned} I_1^{\langle g_s^3 f G^3 \rangle}(n, M^2, \mu) = & -\frac{2m_q}{m_{a_0} f_{a_0}^2} e^{m_{a_0}^2/M^2} \frac{1}{384\pi^2 M^4} \left\{ \delta^{1n} \left[-24 \left(-\ln \frac{M^2}{\mu^2} \right) + 84 \right] + \theta(n-1) \left[-4n(3n-5) \right. \right. \\ & \left. \left. \times \left(-\ln \frac{M^2}{\mu^2} \right) + 2(2n^2+5n-13) \right] + \theta(n-2) \left[-24n^2 \left(-\ln \frac{M^2}{\mu^2} \right) + 2n(n-4)\tilde{\psi}(n) + 17n^2 + 55n + 12 \right] \right. \\ & \left. + \theta(n-3) \left[2n(n-4)\tilde{\psi}(n) + \frac{1}{n-1}(19n^3-32n^2+7n+6) \right] \right\}, \end{aligned} \quad (15)$$

$$I_1^{\langle g_s \bar{q} \sigma T G q \rangle}(n, M^2) = -\frac{1}{m_{a_0} f_{a_0}^2} e^{m_{a_0}^2/M^2} \frac{4n}{3M^2}, \quad (16)$$

with $\tilde{\psi}(n) = \psi(\frac{n+1}{2}) - \psi(\frac{n}{2}) + (-1)^n \ln 4$. It is worth to point out that the detailed terms $\mathcal{B}_{M^2} I_{ijk(n)}$ are listed

in the Appendix A. For a more thorough considering the sum rule for $\langle \xi_{2;a_0}^n \rangle |_\mu$, it might be convenient to calcu-

late $\langle \xi_{3;a_0}^{p;0} \rangle|_\mu$. To achieve this target, one can use the correlator.

$$\Pi_{3;a_0}^{(0,0)}(z, q) = i \int d^4x e^{iq \cdot x} \langle 0 | T \{ J_0^S(x), J_0^{S\dagger}(0) \} | 0 \rangle, \quad (17)$$

for the $a_0(980)$ -meson twist-3 LCDA 0_{th} moment. Followed by the basic procedure of the QCDSR, the expression of the 0_{th} moment of scalar meson $a_0(980)$ -meson twist-3 LCDA can be obtained,

$$\begin{aligned} \langle \xi_{3;a_0}^{p;0} \rangle|_\mu &= I_2^{\text{pert.}}(n, s_0, M^2) \\ &+ \langle \bar{q}q \rangle I_2^{\langle \bar{q}q \rangle}(M^2) \\ &+ \langle g_s \bar{q}q \rangle^2 I_2^{\langle g_s \bar{q}q \rangle^2}(M^2) \\ &+ \langle g_s^2 \bar{q}q \rangle^2 I_2^{\langle g_s^2 \bar{q}q \rangle^2}(M^2, \mu) \\ &+ \langle \alpha_s G^2 \rangle I_2^{\langle \alpha_s G^2 \rangle}(M^2) \\ &+ \langle g_s \bar{q} \sigma T G q \rangle I_2^{\langle g_s \bar{q} \sigma T G q \rangle}(M^2). \end{aligned} \quad (18)$$

In which, the light quark is taken as $q = (u, d)$ and corresponding vacuum condensates are given in the next Section. The detailed expressions for the subitems in Eq. (18) are present as follows,

$$I_2^{\text{pert.}}(s_0, M^2) = \frac{3e^{m_{a_0}^2/M^2} M^2}{8\pi^2 m_{a_0}^2 f_{a_0}^2} \left[M^2 - (M^2 + s_0) e^{-s_0/M^2} \right], \quad (19)$$

$$I_2^{\langle \bar{q}q \rangle}(M^2) = \frac{3m_q e^{m_{a_0}^2/M^2}}{m_{a_0}^2 f_{a_0}^2}, \quad (20)$$

$$I_2^{\langle g_s \bar{q}q \rangle^2}(M^2) = -\frac{8e^{m_{a_0}^2/M^2}}{27m_{a_0}^2 f_{a_0}^2 M^2}, \quad (21)$$

$$I_2^{\langle g_s^2 \bar{q}q \rangle^2}(M^2, \mu) = \frac{e^{m_{a_0}^2/M^2} (2 + \kappa^2)}{486\pi^2 m_{a_0}^2 f_{a_0}^2 M^2} \left[35 - 6 \left(-\ln \frac{M^2}{\mu^2} \right) \right], \quad (22)$$

$$I_2^{\langle \alpha_s G^2 \rangle}(M^2) = \frac{e^{m_{a_0}^2/M^2}}{m_{a_0}^2 f_{a_0}^2} \frac{1}{8\pi}, \quad (23)$$

$$I_2^{\langle g_s \bar{q} \sigma T G q \rangle}(M^2) = \frac{e^{m_{a_0}^2/M^2}}{m_{a_0}^2 f_{a_0}^2 M^2}. \quad (24)$$

Since higher-order and higher-dimensional corrections are difficult to calculate completely, the moments $\langle \xi_{2;a_0}^n \rangle|_\mu$ of the sum rule (9) cannot be normalized in the whole Borel parameter region. To get a more accurate moments $\langle \xi_{2;a_0}^n \rangle|_\mu$ for sum rule, we can use the following expression

$$\langle \xi_{2;a_0}^n \rangle|_\mu = \frac{\langle \xi_{2;a_0}^n \rangle|_\mu \langle \xi_{3;a_0}^{p;0} \rangle|_\mu}{\sqrt{\langle \xi_{3;a_0}^{p;0} \rangle^2|_\mu}} \quad (25)$$

This method can eliminate the systematic errors caused by many factors. The discussion for the pion and kaon cases can be found in our previous work [38, 39].

TABLE I: The expressions of the spin-space wave function $\chi_{2;a_0}^{\lambda_1 \lambda_2}(x, \mathbf{k}_\perp)$ with different $\lambda_1 \lambda_2$.

$\lambda_1 \lambda_2$	$\chi_{2;a_0}^{\lambda_1 \lambda_2}(x, \mathbf{k}_\perp)$	$\lambda_1 \lambda_2$	$\chi_{2;a_0}^{\lambda_1 \lambda_2}(x, \mathbf{k}_\perp)$
$\downarrow\downarrow$	$-\frac{k_x + ik_y}{\sqrt{2(\hat{m}_q^2 + \mathbf{k}_\perp^2)}}$	$\uparrow\uparrow$	$-\frac{k_x - ik_y}{\sqrt{2(\hat{m}_q^2 + \mathbf{k}_\perp^2)}}$
$\uparrow\downarrow$	$+\frac{\hat{m}_q}{\sqrt{2(\hat{m}_q^2 + \mathbf{k}_\perp^2)}}$	$\downarrow\uparrow$	$-\frac{\hat{m}_q}{\sqrt{2(\hat{m}_q^2 + \mathbf{k}_\perp^2)}}$

Normally, conformal expansion of LCDAs Gegenbauer polynomials makes the higher-order Gegenbauer moments unreliable. To improve this situation, the LCHO is adopted to determine $a_0(980)$ -meson twist-2 LCDA. Referring to the LCHO model of the pion leading-twist WF raised in Refs. [40, 41], it is expressed as:

$$\Psi_{2;a_0}(x, \mathbf{k}_\perp) = \sum_{\lambda_1 \lambda_2} \chi_{2;a_0}^{\lambda_1 \lambda_2}(x, \mathbf{k}_\perp) \Psi_{2;a_0}^R(x, \mathbf{k}_\perp) \quad (26)$$

where \mathbf{k}_\perp is transverse momentum. Furthermore, λ_1 and λ_2 are the helicities of the two constituent quark. $\chi_{2;a_0}^{\lambda_1 \lambda_2}(x, \mathbf{k}_\perp)$ stands for the spin-space WF that comes from the Wigner-Melosh rotation. The different forms of $\lambda_1 \lambda_2$ are shown in Table I, which can also be seen in Refs. [42–45]. The spin-space WF, e.g. $\sum_{\lambda_1 \lambda_2} \chi_{2;a_0}^{\lambda_1 \lambda_2}(x, \mathbf{k}_\perp) = \hat{m}_q^2 / (\mathbf{k}_\perp^2 + \hat{m}_q^2)^{1/2}$. Then, by combing the spatial WF $\Psi_{2;a_0}^R(x, \mathbf{k}_\perp) = A_{2;a_0} \varphi_{2;a_0}(x) \exp[-(\mathbf{k}_\perp^2 + \hat{m}_q^2)/(8\beta_{2;a_0}^2 x \bar{x})]$, the $a_0(980)$ -meson WF will be obtained. In which, the $A_{2;a_0}$, \hat{m}_q stand for the normalization constant and light quark mass. The final $a_0(980)$ -meson twist-2 LCDA can be obtained by using the relationship between the twist-2 LCDA and WF of $a_0(980)$ -meson, e.g integrated over the squared transverse momentum, which can be expressed as

$$\begin{aligned} \phi_{2;a_0}(x, \mu) &= \frac{A_{2;a_0} \hat{m}_q \beta_{2;a_0}}{4\sqrt{2}\pi^{3/2}} \sqrt{x\bar{x}} \varphi_{2;a_0}(x) \\ &\times \left\{ \text{Erf} \left[\sqrt{\frac{\hat{m}_q^2 + \mu^2}{8\beta_{2;a_0}^2 x \bar{x}}} \right] - \text{Erf} \left[\sqrt{\frac{\hat{m}_q^2}{8\beta_{2;a_0}^2 x \bar{x}}} \right] \right\}, \end{aligned} \quad (27)$$

where $\text{Erf}(x) = 2 \int_0^x e^{-t^2} dt / \sqrt{\pi}$ is the error function, and $\varphi_{2;a_0}(x) = (x\bar{x})^{\alpha_{2;a_0}} C_1^{3/2}(2x - 1)$. Based on the experience of other mesons [31, 38, 39, 46–51], we take the wavefunction parameter $\beta_{2;a_0} = 0.5$. Whether the value of $\beta_{2;a_0}$ is accurate can be judged by goodness of fit P_{χ^2} . The free parameters $\alpha_{2;a_0}$ and $A_{2;a_0}$ can be obtained by fitting the moments $\langle \xi_{2;a_0}^n \rangle|_\mu$ directly.

In deriving the complete expression for $D \rightarrow a_0(980)$ TFFs, one can take the following correlator

$$\Pi_\mu(p, q) = i \int d^4x e^{iq \cdot x} \langle a_0 | T \{ J_n(x), j_n^\dagger(0) \} | 0 \rangle \quad (28)$$

with $J_n(x) = \bar{q}_1(x)\gamma_\mu\gamma_5 c(x)$, $j_n^\dagger(0) = \bar{c}i\gamma_5 q_2(0)$. Followed by the standard LCSR approach, one can make the OPE near the light-cone in the space-like region, and insert a complete set of $a_0(980)$ -meson states in the physical region. After performing the Borel transformation, we can get the $D \rightarrow a_0(980)$ TFFs $f_\pm^{D \rightarrow a_0}(q^2)$ up to twist-3 accuracy, which can be read off

$$f_+^{D \rightarrow a_0}(q^2) = \frac{m_c f_{a_0}}{m_D^2 f_D} \int_{u_0}^1 du e^{(m_{a_0}^2 - s(u))/M^2} \left\{ -\frac{m_c}{u} \phi_{2;a_0}(u) + m_{a_0} \phi_{3;a_0}^p(u) + \frac{m_{a_0}}{6} \left[\frac{2}{u} \phi_{3;a_0}^\sigma(u) - \frac{1}{m_c^2 + u^2 m_{a_0}^2 - q^2} \times \left((m_c^2 - u^2 m_{a_0}^2 + q^2) \frac{d\phi_{3;a_0}^\sigma(u)}{du} - \frac{4um_c^2 m_{a_0}^2}{m_c^2 + u^2 m_{a_0}^2 - q^2} \times \phi_{3;a_0}^\sigma(u) \right) \right] \right\} \quad (29)$$

$$f_-^{D \rightarrow a_0}(q^2) = \frac{m_c f_{a_0}}{m_D^2 f_D} \int_{u_0}^1 du e^{(m_{a_0}^2 - s(u))/M^2} \left[\frac{\phi_{3;a_0}^p(u)}{u} + \frac{1}{6u} \frac{d\phi_{3;a_0}^\sigma(u)}{du} \right]. \quad (30)$$

In which the abbreviation $s(u) = (m_b^2 + u\bar{u}m_{a_0}^2 - \bar{u}q^2)/u$ is used. The lower limits of the integration is $u_0 = \{[(s_0 - q^2 - m_{a_0}^2)^2 + 4m_{a_0}^2(m_c^2 - q^2)]^{1/2} - (s_0 - q^2 - m_{a_0}^2)\}/(2m_{a_0}^2)$. Here, m_D and f_D are the mass and decay constant of D -meson, m_c is the c -quark mass, $\bar{u} = (1 - u)$, s_0 stands for the continuum threshold. $\phi_{2;a_0}$ and $\phi_{3;a_0}^\sigma$, $\phi_{3;a_0}^p$ are twist-2 and twist-3 LCDAs, respectively. The twist-3 LCDA can be found in Refs. [52, 53]. Then, the decay widths and branching ratio for the semileptonic decay $D \rightarrow a_0(980)\ell\bar{\nu}_\ell$ can be written as [15, 16]

$$\frac{d\Gamma(D \rightarrow a_0(980)\ell\bar{\nu}_\ell)}{dq^2} = \frac{G_F^2 |V_{cb}|^2}{768\pi^3 m_D^3} \frac{(q^2 - m_\ell^2)^2}{q^6} \left[(m_D^2 + m_{a_0}^2 - q^2)^2 - 4m_D^2 m_{a_0}^2 \right]^{1/2} \left\{ \left[(q^2 + m_{a_0}^2 - m_D^2)^2 (q^2 + 2m_\ell^2) - q^2 m_{a_0}^2 (4q^2 + 2m_\ell^2) \right] (f_+^{D \rightarrow a_0}(q^2))^2 + 6q^2 m_\ell^2 (m_D^2 - m_{a_0}^2 - q^2) f_+^{D \rightarrow a_0}(q^2) f_-^{D \rightarrow a_0}(q^2) + 6q^4 m_\ell^2 (f_-^{D \rightarrow a_0}(q^2))^2 \right\}, \quad (31)$$

where m_ℓ , $|V_{cd}|$ and G_F stand for leptonic mass, CKM matrix element and fermi coupling constant.

III. NUMERICAL ANALYSIS

To do the numerical analysis, we adopt meson's mass $m_{a_0(980)} = 0.980 \pm 0.020$ GeV, $m_D = 1.865$ GeV and $m_{D^0} = 1.870$ GeV. Besides, the current quark-mass are $m_u = 2.16_{-0.26}^{+0.49}$ MeV and $m_d = 4.67_{-0.17}^{+0.48}$ MeV at scale $\mu = 2$ GeV. The $a_0(980)$ -meson decay constant is $f_{a_0} = 0.409_{-0.023}^{+0.022}$ GeV and mass of the current charm-quark is

$m_c = 1.237 \pm 0.02$ GeV at scale $\mu = 1.4$ GeV. The values of the non-perturbative vacuum condensates appearing in the BFTSR are given below as [38, 54, 55],

$$\begin{aligned} \langle \bar{q}q \rangle &= (-2.417_{-0.114}^{+0.227}) \times 10^{-2} \text{ GeV}^3 \\ \langle g_s \bar{q}\sigma T G q \rangle &= (-1.934_{-0.103}^{+0.188}) \times 10^{-2} \text{ GeV}^5 \\ \langle g_s \bar{q}q \rangle^2 &= (2.082_{-0.697}^{+0.734}) \times 10^{-3} \text{ GeV}^6 \\ \langle g_s^2 \bar{q}q \rangle^2 &= (7.420_{-2.483}^{+2.614}) \times 10^{-3} \text{ GeV}^6 \\ \langle \alpha_s G^2 \rangle &= 0.038 \pm 0.011 \text{ GeV}^4 \\ \langle g_s^3 f G^3 \rangle &\simeq 0.045 \text{ GeV}^6 \\ \kappa &= 0.74 \pm 0.03 \end{aligned} \quad (32)$$

where the quark-gluon mixed condensate is $\langle g_s \bar{q}\sigma T G q \rangle = m_0^2 \langle \bar{q}q \rangle$ with $m_0^2 = 0.80 \pm 0.02$ GeV². The values of the double-quark condensate $\bar{q}q$, quark-gluon mixed condensate $\langle g_s \bar{q}\sigma T G q \rangle$, four-quark condensate $\langle g_s^2 \bar{q}q \rangle^2$, double-gluon condensate $\langle \alpha_s G^2 \rangle$ and triple-gluon condensate $\langle g_s^3 f G^3 \rangle$ are at $\mu = 2$ GeV. Otherwise, these parameters can be calculated to any scale according to the evolution equation.

In the context of BFTSR, there are two important parameters the continuous threshold s_{a_0} and the Borel parameter M^2 , respectively. We generally take the scale $\mu = M$. Under the 3-loop approximate solution, the $\Lambda_{\text{QCD}}^{(n_f)} \simeq (324, 286, 207)$ MeV for the number of quark flavors $n_f = 3, 4, 5$, with which the $\alpha_s(M_Z) = 0.1179(10)$, $m_c(\bar{m}_c) = 1.27(2)$ GeV, $m_b(\bar{m}_b) = 4.18_{-0.02}^{+0.03}$ GeV and $M_Z = 91.1876(21)$ GeV are used. Furthermore, the gluon or quark vacuum condensates and non-perturbative matrix element at initial scale can be running to other scales thought out the renormalization group equations (RGE) [56, 57], which can be written as a general formula:

$$\chi(\mu) = \left[\frac{\alpha_s(\mu_0)}{\alpha_s(\mu)} \right]^{y(n_f)} \chi(\mu_0) \quad (33)$$

with which the function $y(n_f)$ are $-4/b$, $-4/b$ and $-2/(3b)$ for the m_q , $\langle \bar{q}q \rangle$ and $\langle g_s \bar{q}\sigma T G q \rangle$, respectively. The coefficient $b = (33 - 2n_f)/3$ and n_f is the number of active quark flavors. According to the basic assumption of BFTSR, it is worth noting that g_s is the coupling constant between background fields in the above vacuum condensates, which is different from the coupling constant in pQCD and should be absorbed into the vacuum condensates as part of these non-perturbative parameters. The RGE of the Gegenbauer moments of the $a_0(980)$ -meson twist-2 LCDA is [18]:

$$a_n^{2;a_0}(\mu) = a_n^{2;a_0}(\mu_0) E_n(\mu, \mu_0), \quad (34)$$

with $E_n(\mu, \mu_0) = [\alpha_s(\mu)/\alpha_s(\mu_0)]^{-(\gamma_n^{(0)} + 4)/(b)}$. The μ_0 and μ represent the initial scale and the running scale, the one-loop anomalous dimensions is $\gamma_n^{(0)} = C_F \{ [1 - 2/((n+1)(n+2))] + 4 \sum_{j=2}^{n+1} 1/j \}$, with $C_F = 4/3$. According to the RGE of the Gegenbauer moments, one can

TABLE II: The determined Borel windows and the corresponding $a_0(980)$ -meson twist-2 LCDA moments $\langle \xi_{2;a_0}^n \rangle|_\mu$ with $n = (1, 3, 5, 7, 9)$ at the scale $\mu_k = 1.4$ GeV. Where all input parameters are set to be their central values. In which the abbreviation “Con.” indicate the continuum contributions.

n	M^2	$\langle \xi_{2;a_0}^n \rangle _\mu$	Con.
1	[2.483, 3.483]	[-0.250, -0.203]	< 30%
3	[1.869, 2.869]	[-0.095, -0.129]	< 20%
5	[3.057, 4.057]	[-0.041, -0.074]	< 40%
7	[4.143, 5.143]	[-0.020, -0.048]	< 60%
9	[4.916, 5.916]	[-0.000, -0.027]	< 75%

get the moments $\langle \xi_{2;a_0}^n \rangle|_\mu$ for the arbitrary scale μ .

Furthermore, the continuum threshold parameter for the sum rule $\langle \xi_{2;a_0}^n \rangle|_\mu$ can be determined by normalization for $\langle \xi_{3;a_0}^{p;0} \rangle|_\mu$, which leads to $s_{a_0} = 7$ GeV². Then, the Borel window for the each order of $a_0(980)$ -meson LCDA moments can be determined by limiting the continuum states and the dimension-six condensates contributions. Then, the moments $\langle \xi_{2;a_0}^n \rangle|_\mu$ with $n = (1, 3, 5, 7, 9)$ within uncertainties coming from Borel parameters are listed in Table II. Based on the BFTSR, the dimension-six condensates contributions for $\langle \xi_{2;a_0}^n \rangle|_\mu$ are less than 1% for all the n th-order. To get the suitable Borel window, the continuum contributions for $\langle \xi_{2;a_0}^n \rangle|_\mu$ are restrict to (30, 20, 40, 60, 75)% for $n = (1, 3, 5, 7, 9)$ respectively. Since the dimension-six condensates contributions are very small, we determine the upper limit of the Borel parameter M^2 through the continuum contributions. Then the lower limit of the Borel parameter M^2 can be determined by the method of the upper limits, so as to obtain the appropriate Borel window. At the same time, the values of the moments $\langle \xi_{2;a_0}^n \rangle|_\mu$ are stable in the appropriate Borel window. To have a deeper insight into the relationship of the LCDA moments versus Borel parameter M^2 , the first five moments's curves are shown in Fig. 1, which can be seen that

- In the region $M^2 \in [1, 2]$ of Borel window, the curves for $\langle \xi_{2;a_0}^n \rangle|_\mu$ changed dramatically. With the increase of Borel window M^2 , the change trend of moments $\langle \xi_{2;a_0}^1 \rangle|_\mu$, $\langle \xi_{2;a_0}^3 \rangle|_\mu$, $\langle \xi_{2;a_0}^5 \rangle|_\mu$, $\langle \xi_{2;a_0}^7 \rangle|_\mu$, $\langle \xi_{2;a_0}^9 \rangle|_\mu$ tends to be gentle.
- With n increases, the absolute value of the moments $\langle \xi_{2;a_0}^n \rangle|_\mu$ tend to be smaller.

Taking all the input uncertainties into consideration, we can get the moments $\langle \xi_{2;a_0}^n \rangle|_\mu$ with $n = (1, 3, 5, 7, 9)$ under two types of factorization scale μ_0 and μ_k ,

$$\begin{aligned} \langle \xi_{2;a_0}^1 \rangle|_{\mu_0} &= -0.307(43), & \langle \xi_{2;a_0}^1 \rangle|_{\mu_k} &= -0.247(34), \\ \langle \xi_{2;a_0}^3 \rangle|_{\mu_0} &= -0.181(34), & \langle \xi_{2;a_0}^3 \rangle|_{\mu_k} &= -0.123(22), \\ \langle \xi_{2;a_0}^5 \rangle|_{\mu_0} &= -0.078(28), & \langle \xi_{2;a_0}^5 \rangle|_{\mu_k} &= -0.065(21), \end{aligned}$$

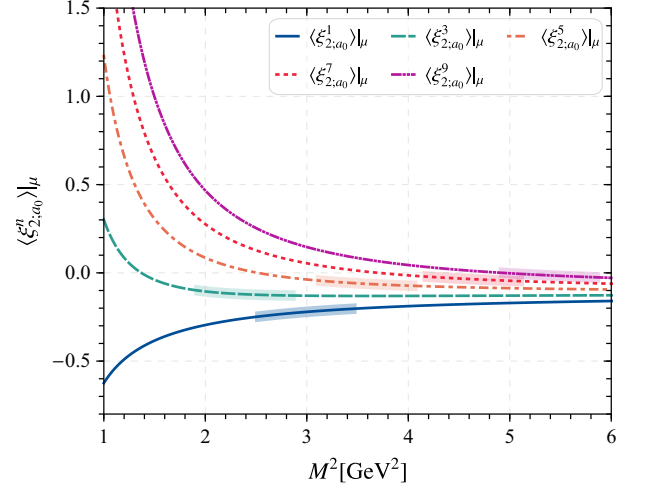


FIG. 1: (Color online) The $a_0(980)$ -meson leading-twist DA moments $\langle \xi_{2;a_0}^n \rangle|_\mu$ with $n = (1, 3, 5, 7, 9)$ versus the Borel parameter M^2 , where all input parameters are set to be their central values. In which, the shaded band indicate the Borel Windows for $n = (1, 3, 5, 7, 9)$, respectively.

$$\begin{aligned} \langle \xi_{2;a_0}^7 \rangle|_{\mu_0} &= -0.049(26), & \langle \xi_{2;a_0}^7 \rangle|_{\mu_k} &= -0.040(19), \\ \langle \xi_{2;a_0}^9 \rangle|_{\mu_0} &= -0.036(24), & \langle \xi_{2;a_0}^9 \rangle|_{\mu_k} &= -0.019(16), \end{aligned} \quad (35)$$

Our results for the first two order are slightly smaller than the Cheng's predictions, e.g. $\langle \xi_{2;a_0}^1 \rangle|_{\mu_0} = -0.56(5)$ and $\langle \xi_{2;a_0}^3 \rangle|_{\mu_0} = -0.21(3)$ by using the QCDSR approach from Ref. [18], which is more likely to be antisymmetric behavior. The little difference may be related to the different methods in determining the continuum threshold s_{a_0} . Meanwhile, the higher order such as $n = (5, 7, 9)$ are given for the first time.

Secondly, the free parameters $\alpha_{2;a_0}$ and $A_{2;a_0}$ for the LCHO model can be fixed by adopting the method of least squares to fit $\langle \xi_{2;a_0}^n \rangle|_\mu$ calculated in the framework of the BFTSR shown in Eq. (35). The goodness of fit can be judged by the probability P_{χ^2} ($P_{\chi^2} \in [0, 1]$)¹. By fitting the moments $\langle \xi_{2;a_0}^n \rangle|_{\mu_k}$ at the scale $\mu_k = 1.4$ GeV, the optimal model parameters are obtained as follows,

$$\begin{aligned} A_{2;a_0} &= -300 \text{ GeV}^{-1}, \\ \alpha_{2;a_0} &= -0.25, \\ \beta_{2;a_0} &= 0.5 \text{ GeV}, \end{aligned} \quad (36)$$

The above parameters are derived from $m_q = 250$ MeV. From these parameters, we obtain the scalar $a_0(980)$ -meson twist-2 LCDA $\phi_{2;a_0}(x, \mu_k)$, which is shown in the left panel of Fig. 2. In the meantime, we also present the results of QCDSR [18] prediction as a comparison. From the perspective of variation trend, our prediction results

¹ For more details, one can see our previous work for pion [38].

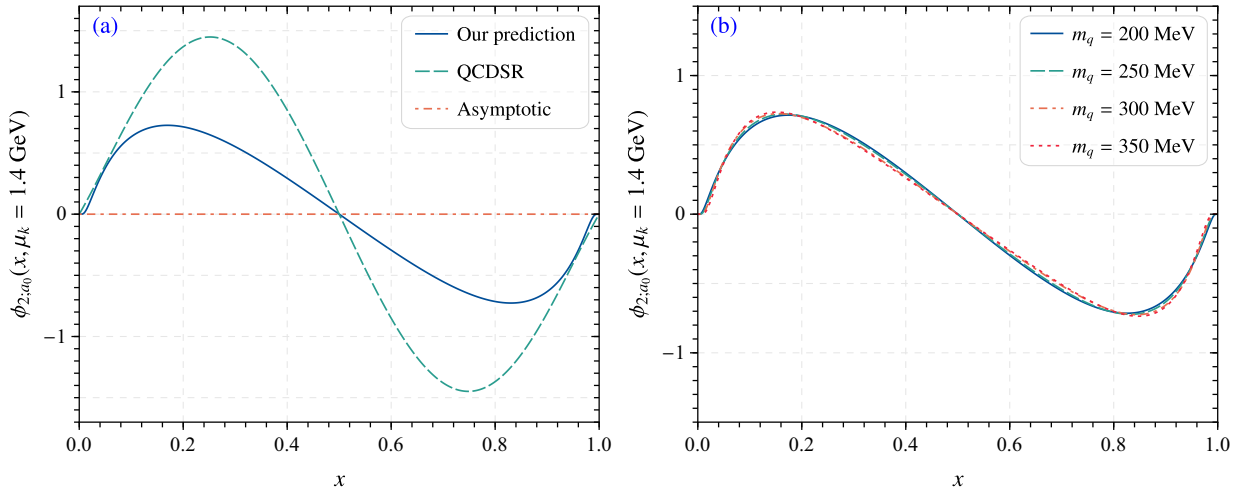


FIG. 2: (Color online) The $a_0(980)$ -meson twist-2 DA curves in this work. As a comparison, we present the curve trend of QCDSR distribution amplitude [18] in the left panel. In the right panel, the $a_0(980)$ -meson twist-2 DA $\phi_{2;a_0}(x, \mu)$ at $\mu_k = 1.4$ GeV with the constituent quark mass $m_q = (200, 250, 300, 350)$ MeV are given, respectively.

TABLE III: The model parameters m_q (in unit: MeV) of LCHO model $\varphi_{2;a_0}^{\text{IV}}(x)$ under different quark masses and their corresponding goodness of fit.

m_q	$A_{2;a_0} (\text{GeV}^{-1})$	$\alpha_{2;a_0}$	$P_{\chi_{\min}^2}$
200MeV	-440	-0.08	0.912
250MeV	-300	-0.25	0.920
300MeV	-190	-0.48	0.928
350MeV	-140	-0.66	0.935

are relatively consistent with the those of QCDSR, and twist-2 LCDA are both antisymmetric. However, there are also some differences between the two, which may be due to differences in calculation methods. The former uses the Gegenbauer moments polynomials expansion, while we take the LCHO model to construct LCDA $\phi_{2;a_0}(x, \mu)$.

For further study, we also analyze the relationship between the goodness-fit of the $a_0(980)$ -meson twist-2 LCDA $\phi_{2;a_0}(x, \mu_k)$ and the quark mass m_q listed in Table III. It is obvious that as the quark mass increases, the goodness of fit also increases. The goodness of fit $P_{\chi_{\min}^2}$ also indicates that $\beta_{2;a_0} = 0.5\text{GeV}$ is reasonable. Considering the effect of quark mass m_q on the $a_0(980)$ -meson twist-2 LCDA $\phi_{2;a_0}(x, \mu_k)$, the behavior of LCHO model $\phi_{2;a_0}(x, \mu)$ for different quark masses $m_q = (200, 250, 300, 350)$ MeV is shown in the right panel of Fig. 2. As can be seen from the figure, the peak value of the LCHO model curves increases with the increase of mass m_q . In addition to this, the relationship between goodness of fit $P_{\chi_{\min}^2}$ and parameters $A_{2;a_0}$ and $\alpha_{2;a_0}$ is also shown in Fig. 3. From the table we can see that the $P_{\chi_{\min}^2}$ can reach to 93%, which shows the fitting is good.

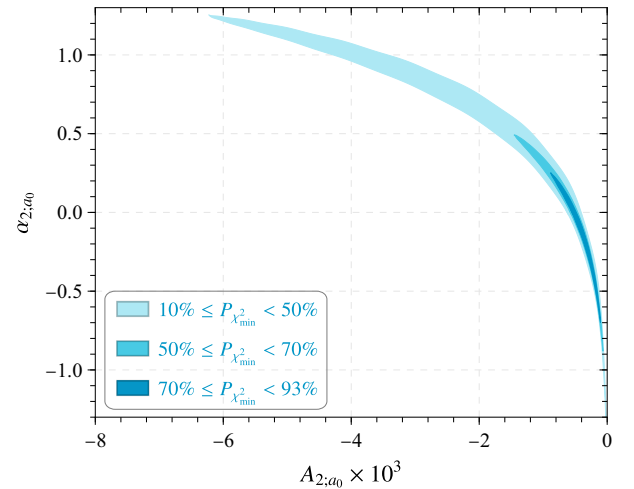


FIG. 3: (Color online) Relationship between the goodness of fit $P_{\chi_{\min}^2}$ and the two LCHO parameters $A_{2;a_0}$, $\alpha_{2;a_0}$. In which the $P_{\chi_{\min}^2}$ is separated into three area with different color.

The TFFs is an important parameter in the calculation of the semileptonic decay $D \rightarrow a_0(980)\ell\bar{\nu}_\ell$. To obtain the numerical results of TFFs, we take $\mu_k = 1.4$ GeV, $m_D = 1.869$ GeV [58], $f_{a_0(980)} = (0.409_{-0.023}^{+0.022})$ GeV [18]. For the continuum threshold s_0 , it is generally taken near the mass square of the first excited state of D -meson, that is, near the mass square of $D(2550)$ -meson. Based on the prediction of the sum rule of heavy quark effective theory (HQET) [59], we take the continuum threshold parameter $s_0 = 6.50(25)$ GeV², which is also agree with Ref. [60].

According to LCSR, in the suitable Borel window, we

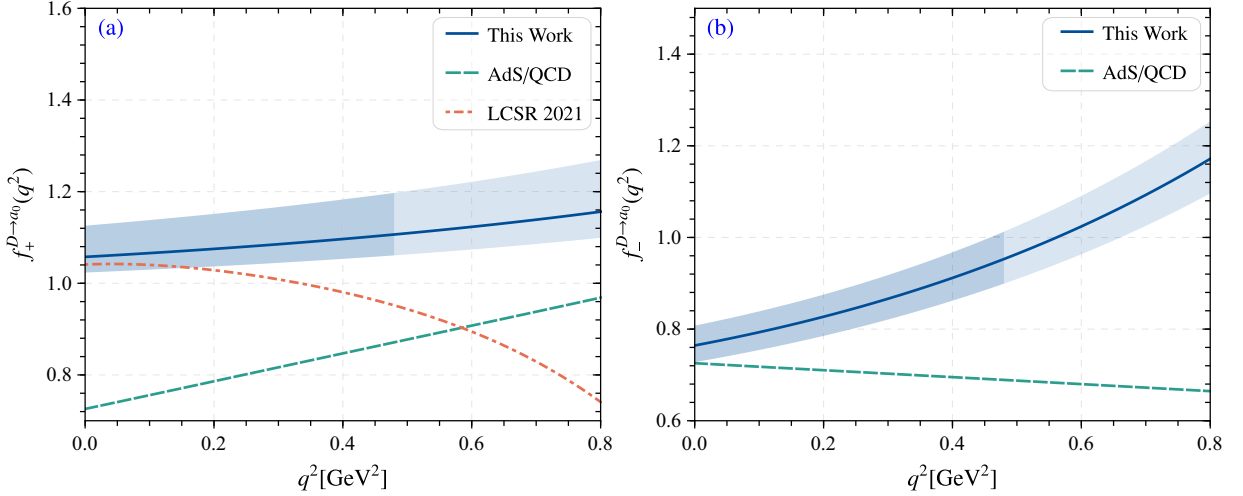


FIG. 4: (Color online) The $D \rightarrow a_0(980)\ell\bar{\nu}_\ell$ TFFs $f_+^{D \rightarrow a_0}(q^2)$ and $f_-^{D \rightarrow a_0}(q^2)$ of our predictions within uncertainties. In which, the darker band stand for the results calculated in LCSR, and the light colored band stand for the SSE. Meanwhile, the results for LCSR [16] and AdS/QCD [17] as a comparison.

TABLE IV: TFFs at the point of large recoil $q^2 \simeq 0$ for $D \rightarrow a_0(980)$ within uncertainties. And a comparison with other theoretical groups are also given.

	$f_+^{D \rightarrow a_0}(0)$	$f_-^{D \rightarrow a_0}(0)$
This work	$1.058_{-0.035}^{+0.068}$	$0.764_{-0.036}^{+0.044}$
CCQM [14]	$0.55_{-0.02}^{+0.02}$	$0.03_{-0.01}^{+0.01}$
LCSR 2021 [16]	$0.85_{-0.11}^{+0.10}$	$-0.85_{-0.11}^{+0.10}$
LCSR 2017 [15]	1.76(26)	0.31(13)
AdS/QCD [17]	0.72(9)	-

predict the end values of the $D \rightarrow a_0(980)\ell\bar{\nu}_\ell$ semileptonic decay TFFs shown in Table IV. As a comparison, the results predicted from various approaches, CCQM [14], LCSR 2017 [15], LCSR 2021 [16] and AdS/QCD [17] also are presented in Table IV. It is not difficult to see from the Table IV that our predicted results are significantly different from those obtained by other predictions. The reason lies in the twist-2 LCDA $\phi_{2,a_0}(x, \mu)$ is different, which the LCHO model is used here.

In the physical sense, the LCSR method is suitable for in low and intermediate q^2 region. The physical region for $D \rightarrow a_0(980)$ TFFs is $m_e \leq q^2 \leq 0.48 \text{ GeV}^2$. In order to obtain reasonable LCSR results, we can extend them to the entire physical q^2 -region $m_e \leq q^2 \leq (m_D^2 - m_{a_0})^2 = 0.8 \text{ GeV}^2$. Therefore, we can fit the complete analysis results with simplified series expansion (SSE), which is a rapidly convergent series on the $z(t)$ -expansion [61–63].

$$f_i(q^2) = P_i(q^2) \sum_{k=0,1,2} a_k^i [z(q^2) - z(0)]^k, \quad (37)$$

where $f_i(q^2)$ stands for $D \rightarrow a_0(980)\ell\bar{\nu}_\ell$ TFFs, a_k^i the fit

TABLE V: The fitting parameters a_i with $i = (1, 2)$ for TFFs $f_+^{D \rightarrow a_0}(q^2)$ and $f_-^{D \rightarrow a_0}(q^2)$. In which, the goodness of fit Δ are also present.

$f_+^{D \rightarrow a_0}(q^2)$	Central value	Upper limits	Lower limits
a_1	7.279	6.686	7.562
a_2	33.88	38.93	30.14
Δ	0.19%	0.19%	0.19%
$f_-^{D \rightarrow a_0}(q^2)$	Central value	Upper limits	Lower limits
a_1	-1.556	-1.776	-1.178
a_2	147.1	167.9	129.1
Δ	0.29%	0.33%	0.25%

coefficients, and

$$P_i(q^2) = \left(1 - \frac{q^2}{m_{R,i}^2}\right)^{-1} \quad (38)$$

$$z(t) = \frac{\sqrt{t_+ - t} - \sqrt{t_+ - t_0}}{\sqrt{t_+ - t} + \sqrt{t_+ - t_0}}$$

with $t_{\pm} \equiv (m_D \pm m_{a_0})^2$, $t_0 = t_+(1 - \sqrt{1 - t_-/t_+})$. $P_i(q^2)$ is a simple pole corresponding to the first resonance in the spectrum. The fitting parameters a_i for the TFFs within uncertainties are given in Table V. Meanwhile, the goodness of fit $\Delta = \sum_t |F_i(t) - F_i^{\text{fit}}(t)| / \sum_t |F_i(t)| \times 100$ with $t \in [0, 1/100, \dots, 100/100] \times 0.48 \text{ GeV}$ for each TFFs are also presented. After extrapolating TFFs to the whole q^2 region, the curves $f_{\pm}^{D \rightarrow a_0}(q^2)$ are shown in the Fig. 4. We also give the curves obtained by LCSR 2021 [16] and AdS/QCD [17] for comparison. The results show our prediction is a certain discrepancy between the results in Ref. [16]. There are also some deviations from results

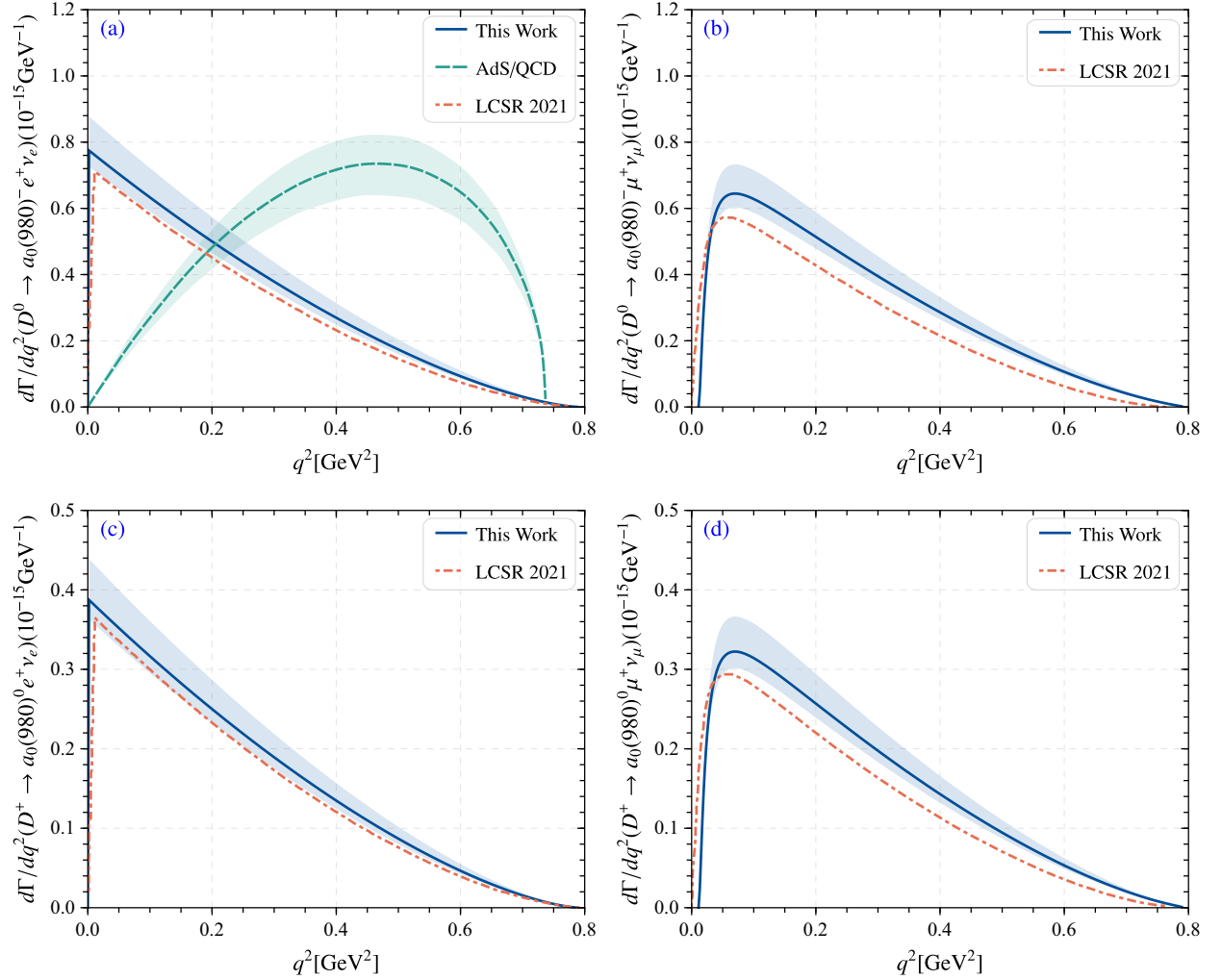


FIG. 5: (Color online) The differential decay widths for $D \rightarrow a_0(980)\ell\bar{\nu}_\ell$ with $\ell = (e, \mu)$ decay process within uncertainties. In which, the LCSR [16] and AdS/QCD [17] predictions are also presented.

predicted by AdS/QCD, but the curve trend is relatively consistent. In most cases, The $f_+^{D \rightarrow a_0}(q^2)$ shows an upward trend with the increase of q^2 . Our prediction is quite reasonable. The $f_-^{D \rightarrow a_0}(q^2)$ is also exhibit upward tendency and it turns out that there are some differences.

As other important parameters for $D \rightarrow a_0(980)\ell\bar{\nu}_\ell$, the CKM matrix element $|V_{cd}| = 0.221 \pm 0.008$ from the PDG [58], the fermi coupling constant $G_F = 1.166 \times 10^{-5} \text{ GeV}^{-2}$. By taking the derived $D \rightarrow a_0(980)\ell\bar{\nu}_\ell$ TFFs and the related parameters into the differential decay widths Eq. (31), one can get the differential decay widths of $D \rightarrow a_0(980)\ell\bar{\nu}_\ell$ with $\ell = (e, \mu)$ presented in Fig. 5. For comparison, we also present the results of LCSR 2021 [16] predictions in Fig. 5. The figure shows that our prediction is consistent with the result of LCSR 2021 within a certain error range. In Fig. 5(a), discrepancy between our prediction and the result of AdS/QCD, which may be caused by the different TFFs. Obviously, the predicted results converge to zero in the small recoil

region $q^2 = (m_D - m_{a_0})^2$. The shaded part in the figure is the error of the width, which mainly comes from the uncertainty of all parameters.

Furthermore, by taking the lifetimes of D^0 , D^+ meson $\tau_{D^0} = (0.410 \pm 0.001)\text{ps}$ and $\tau_{D^+} = (1.033 \pm 0.005)\text{ps}$ from PDG, we can obtain the branching ratio of semileptonic decay channels $D^+ \rightarrow a_0(980)^0 \ell^+ \nu_\ell$ ($\ell = e, \mu$) and $D^0 \rightarrow a_0(980)^- \ell^+ \nu_\ell$ in Table VI. What's more, the predictions from theoretical groups such as CCQM [14], LCSR [15, 16], AdS/QCD [17] are shown in Table VI. It is obvious that our results are relatively consistent with those of CCQM and LCSR 2021 within the error. However, the significant difference between our predictions and LCSR 2017, AdS/QCD may be caused by the difference of the TFFs and $a_0(980)$ -meson twist-2 LCDA.

Additionally, we also calculate the absolute branching ratio of decays $D \rightarrow \eta\pi\ell\bar{\nu}_\ell$ by using the relationship

$$\mathcal{B}(D \rightarrow a_0(980)(\rightarrow \eta\pi)e^+\nu_e) =$$

TABLE VI: Branching fractions for the four different channels of $D \rightarrow a_0(980)\ell\bar{\nu}_\ell$ (in unit: 10^{-4}). To make a comparison, we also listed the CCQM [14], LCSR [15, 16] and AdS/QCD [17] predictions.

	$D^0 \rightarrow a_0(980)^- e^+ \nu_e$	$D^0 \rightarrow a_0(980)^- \mu^+ \nu_\mu$	$D^+ \rightarrow a_0(980)^0 e^+ \nu_e$	$D^+ \rightarrow a_0(980)^0 \mu^+ \nu_\mu$
This work	$1.529^{+0.230}_{-0.108}$	$1.452^{+0.220}_{-0.105}$	$1.927^{+0.288}_{-0.137}$	$1.830^{+0.277}_{-0.130}$
CCQM [14]	1.68 ± 0.15	1.63 ± 0.14	2.18 ± 0.38	2.12 ± 0.37
LCSR 2017 [15]	$4.08^{+1.37}_{-1.22}$	-	$5.40^{+1.78}_{-1.59}$	-
LCSR 2021 [16]	1.36	1.21	1.79	1.59
AdS/QCD [17]	2.44 ± 0.30	-	-	-

TABLE VII: The absolute branching ratio of $D \rightarrow a_0(980)(\rightarrow \eta\pi)e^+\nu_e$ (unit: 10^{-4}) of our predictions within uncertainties. To make a comparison, we also listed the BESIII collaboration [12], LCSR results [16] and PDG average value [58].

	$\mathcal{B}(D^0 \rightarrow a_0(980)^- (\rightarrow \eta\pi^-) e^+ \nu_e)$	$\mathcal{B}(D^+ \rightarrow a_0(980)^0 (\rightarrow \eta\pi^0) e^+ \nu_e)$
This work	$1.292^{+0.194}_{-0.092}$	$1.628^{+0.244}_{-0.116}$
BESIII [12]	$1.33^{+0.33}_{-0.29}$	$1.66^{+0.81}_{-0.66}$
LCSR 2021 [16]	1.15	1.51
PDG [58]	$1.33^{+0.30}_{-0.29}$	$1.7^{+0.8}_{-0.7}$

$$\mathcal{B}(D \rightarrow a_0(980)e^+\nu_e) \times \mathcal{B}(a_0(980) \rightarrow \eta\pi). \quad (39)$$

In which the $\mathcal{B}(a_0(980)^0 \rightarrow \eta\pi^0) = \mathcal{B}(a_0(980)^- \rightarrow \eta\pi^-) = 0.845 \pm 0.017$ can be used [18]. Combing with the $\mathcal{B}(D \rightarrow a_0(980)e^+\nu_e)$ been calculated in this paper, we can get the results for $\mathcal{B}(D^0 \rightarrow a_0(980)^- (\rightarrow \eta\pi^-) e^+ \nu_e)$ and $\mathcal{B}(D^+ \rightarrow a_0(980)^0 (\rightarrow \eta\pi^0) e^+ \nu_e)$, which are listed in Table VII. For comparison, the results of the BESIII [12] collaboration, theory groups LCSR 2021 [16] and PDG [58] predictions are also given. The results show that our predicted absolute branching ratio are in good agreement with those predicted of BESIII, LCSR 2021 and PDG within the error range. It is clear that our prediction is more accurate than the LCSR 2021 prediction, with an improvement of about 12%. It shows that the result of our prediction is reasonable.

IV. SUMMARY

In this paper, we have calculated the moments of $a_0(980)$ -meson twist-2 LCDA by adopting the QCDSR approach within the background field theory. The continuum threshold parameter s_{a_0} is determined from the normalization for the $a_0(980)$ -meson twist-3 LCDA 0_{th}-order moments. After seeking the suitable Borel windows, we present the first five order moments, i.e. $\langle \xi_{2;a_0}^n \rangle|_\mu$ with $n = (1, 3, 5, 7, 9)$ under two different factorization scale μ_0 and μ_k . Then, we study $a_0(980)$ -meson twist-2 LCDA $\phi_{2;a_0}(x, \mu)$ based on the LCHO model for improving the accuracy of the calculation. The least square method is used to fit the moments $\langle \xi_{2;a_0}^n \rangle|_\mu$ and to determine the model parameters. The goodness of fit can be up to 93%. Then, the curves of $a_0(980)$ -meson twist-2 LCDA com-

paring with other theoretical groups and with different constituent quark masses are presented.

The $D \rightarrow a_0(980)$ TFFs are calculated within the LCSR approach. The TFFs at large recoil region are listed in Table IV. After extrapolating the TFFs to the whole q^2 region, the curves $f_\pm^{D \rightarrow a_0}(q^2)$ are shown in Fig. 4. A comparison of TFFs with other LCSR and AdS/QCD predictions are also given. Using the resultant TFFs, we further studied the semileptonic decays $D \rightarrow a_0(980)\ell\bar{\nu}_\ell$ with $\ell = (e, \mu)$. Their differential decay widths are presented in Fig. 5, and their branching fractions are given in Table VI. The ratio of partial branching fractions is given

$$\frac{\mathcal{B}(D^0 \rightarrow a_0(980)^- e^+ \nu_e)}{\mathcal{B}(D^+ \rightarrow a_0(980)^0 e^+ \nu_e)} = 0.793^{+0.180}_{-0.159}, \quad (40)$$

which agree with the CCQM prediction [14] and the LCSR predictions [15, 16] within errors.

After considering the decay $a_0(980) \rightarrow \eta\pi$, we have calculated the branching fractions for the decay processes $D \rightarrow \eta\pi e^+\nu_e$, $\mathcal{B}(D^0 \rightarrow \eta\pi^- e^+ \nu_e) = (1.292^{+0.194}_{-0.092}) \times 10^{-4}$ and $\mathcal{B}(D^+ \rightarrow \eta\pi^0 e^+ \nu_e) = (1.628^{+0.244}_{-0.116}) \times 10^{-4}$. These results are consistent with the BESIII data and the PDG average value within errors. Along with other results of branching fraction for scalar meson discovered experimentally, we will have a reliable input for understanding the nature of the light scalar mesons.

Acknowledgments

Hai-Bing Fu and Tao Zhong would like to thank the Institute of Theoretical Physics in Chongqing University

for kind hospitality. This work was supported in part by the National Natural Science Foundation of China under Grant No.12265010, No.12265009, No.12175025 and No.12147102, the Project of Guizhou Provincial Department of Science and Technology under Grant No.ZK[2021]024, the Project of Guizhou Provincial Department of Education under Grant No.KY[2021]030, and by the Chongqing Graduate Research and Innovation Foundation under Grant No. ydstd1912.

tudes. In which the partial result of the first term of Eq. (5) are given as follows with the form of $\mathcal{B}_{M^2} I_{ijk(n)}$. The subscripts number i, j, k stand for the dimension of propagators and vertex operators respectively, and n represents the n -th term of $\mathcal{B}_{M^2} I_{ijk}$.

Appendix A: Detailed expressions for $I_{2;a_0}^{(n,0)}(n, M^2)$ in BFTSR for $\langle \xi_{2;a_0}^n \rangle|_\mu$

Based on the BFTSR, we calculate the moments $\langle \xi_{2;a_0}^n \rangle|_\mu$ of $a_0(980)$ -meson twist-2 distribution ampli-

$$\mathcal{B}_{M^2} I_{004(0)} = \frac{\langle \alpha_s G^2 \rangle}{8\pi M^4} m_q \left[(-1)^n \left((2n+1) \left(-\ln \frac{M^2}{\mu^2} \right) - n - 2 \right) + \theta(n-2) \left(\frac{2n+1}{2} \tilde{\psi}(n) - (n+1) \frac{(-1)^n n + 1}{n} \right) \right], \quad (\text{A1})$$

$$\mathcal{B}_{M^2} I_{006(1)} = \frac{17 \langle g_s^2 \bar{q}q \rangle^2}{648\pi^2 M^6} m_q \left[-2(-1)^n \delta^{0n} + (-1)^n \theta(n-1) \left(2n \left(-\ln \frac{M^2}{\mu^2} \right) - n - 3 \right) + \theta(n-2) \left(n \tilde{\psi}(n) - (-1)^n n - 1 \right) \right], \quad (\text{A2})$$

$$\mathcal{B}_{M^2} I_{006(2)} = \frac{88 \langle g_s^2 \bar{q}q \rangle^2 - 81 \langle g_s^3 f G^3 \rangle}{2592\pi^2 M^6} m_q \left\{ -(-1)^n \frac{\delta^{0n}}{2} + (-1)^n \left(2n^2 \left(-\ln \frac{M^2}{\mu^2} \right) - \frac{7n^2 + 19n + 2}{4} \right) - \theta(n-3) \left[-n^2 \tilde{\psi}(n) + \frac{1}{4} \left((-1)^n (5n^2 + n) + 4n + 2 \right) \right] \right\}, \quad (\text{A3})$$

$$\mathcal{B}_{M^2} I_{022(0)} = \frac{\langle \alpha_s G^2 \rangle}{24\pi M^4} m_q \left[2(-1)^n \theta(n-1) n \left(-\ln \frac{M^2}{\mu^2} \right) + \theta(n-2) \left(n \tilde{\psi}(n) - (-1)^n - 1 \right) \right], \quad (\text{A4})$$

$$\mathcal{B}_{M^2} I_{024(1)} = \frac{\langle g_s^2 \bar{q}q \rangle^2}{648\pi^2 M^6} m_q \left[2(-1)^n \theta(n-1) \left(n \left(-\ln \frac{M^2}{\mu^2} \right) - 1 \right) + \theta(n-2) n \tilde{\psi}(n) \right], \quad (\text{A5})$$

$$\mathcal{B}_{M^2} I_{024(2)} = \frac{8 \langle g_s^2 \bar{q}q \rangle^2 - 27 \langle g_s^3 f G^3 \rangle}{2592\pi^2 M^6} m_q n \left[(-1)^n \theta(n-1) \left((2n-1) \left(-\ln \frac{M^2}{\mu^2} \right) - n - 3 + \frac{1}{n} \right) + \theta(n-3) \left(\frac{2n-1}{2} \tilde{\psi}(n) - 1 - (-1)^n n \right) \right], \quad (\text{A6})$$

$$\mathcal{B}_{M^2} I_{024(3)} = \frac{\langle g_s^2 \bar{q}q \rangle^2}{972\pi^2 M^6} m_q \left\{ -4(-1)^n n(n-1) \theta(n-2) \left(\left(-\ln \frac{M^2}{\mu^2} \right) - \frac{1}{2} \right) - \theta(n-3) \left(2n(n-1) \tilde{\psi}(n) - ((-1)^n (4n-3) + 2n - 1) \right) \right\} \quad (\text{A7})$$

$$\mathcal{B}_{M^2} I_{024(4)} = \frac{\langle g_s^2 \bar{q}q \rangle^2}{486\pi^2 M^6} m_q \left[2n \delta^{1n} \left(\left(-\ln \frac{M^2}{\mu^2} \right) - 2 \right) - 2(-1)^n n^2 \theta(n-2) \left(\left(-\ln \frac{M^2}{\mu^2} \right) - 1 - \frac{1}{n} \right) - \theta(n-3) \left(n^2 \tilde{\psi}(n) - \frac{1}{2} (-1)^n (2n^2 + 2(1 + (-1)^n) + (-1)^n - 1) \right) \right], \quad (\text{A8})$$

$$\mathcal{B}_{M^2} I_{033(1)} = -\frac{\langle g_s^2 \bar{q}q \rangle^2}{486\pi^2 M^6} m_q \left[2(-1)^n \theta(n-1) \left(n \left(-\ln \frac{M^2}{\mu^2} \right) - 1 \right) + \theta(n-2) n \tilde{\psi}(n) \right], \quad (\text{A9})$$

$$\mathcal{B}_{M^2} I_{033(2)} = \frac{\langle g_s^2 \bar{q}q \rangle^2}{243\pi^2 M^6} m_q n \left[(-1)^n \theta(n-1) \left(4n \left(-\ln \frac{M^2}{\mu^2} \right) - 5 \right) + 2\theta(n-2) \left(n \tilde{\psi}(n) - (-1)^n - 1 \right) \right], \quad (\text{A10})$$

$$\mathcal{B}_{M^2} I_{033(3)} = -\frac{\langle g_s^2 \bar{q}q \rangle^2}{486\pi^2 M^6} m_q n \left[2(-1)^n \theta(n-1) \left(n \left(-\ln \frac{M^2}{\mu^2} \right) - 1 \right) + \theta(n-2) \left(n \tilde{\psi}(n) - (-1)^n - 1 \right) \right], \quad (\text{A11})$$

$$\mathcal{B}_{M^2} I_{042(0)} = -\frac{16 \langle g_s^2 \bar{q}q \rangle^2 + 27 \langle g_s^3 f G^3 \rangle}{5184\pi^2 M^6} m_q n \left[2(-1)^n \theta(n-1) \left(n \left(-\ln \frac{M^2}{\mu^2} \right) - 1 \right) + \theta(n-2) \left(n \tilde{\psi}(n) - (-1)^n - 1 \right) \right], \quad (\text{A12})$$

$$\mathcal{B}_{M^2} I_{202(1)} = \frac{\langle \alpha_s G^2 \rangle}{8\pi M^4} m_q \left[\left(-\ln \frac{M^2}{\mu^2} \right) + \frac{1}{2} (-1)^n \theta(n-1) \left(\tilde{\psi}(n) - \frac{2}{n} \right) \right], \quad (\text{A13})$$

$$\mathcal{B}_{M^2 I_{202(2)}} = -\frac{\langle \alpha_s G^2 \rangle}{8\pi M^4} m_q \left[(-1)^n \left(-\ln \frac{M2}{\mu^2} \right) + \frac{1}{2} \theta(n-1) \left(\tilde{\psi}(n) - \frac{2}{n} \right) \right], \quad (\text{A14})$$

$$\mathcal{B}_{M^2 I_{204(1)}} = \frac{(\langle 8g_s^2 \bar{q}q \rangle^2 + 81 \langle g_s^3 f G^2 \rangle) m_q}{5184\pi^2 M^6} \left\{ -2\delta^{0n} + 2n(-1)^n \theta(n-1) \left(n \left(-\ln \frac{M2}{\mu^2} \right) - \frac{n+3}{2n} \right) + \theta(n-2) \left(\tilde{\psi}(n) - (n + (-1)^n n) \right) \right\}, \quad (\text{A15})$$

$$\mathcal{B}_{M^2 I_{204(2)}} = \frac{\langle g_s^2 \bar{q}q \rangle^2}{972\pi^2 M^6} m_q n \left\{ \left(-2(-1)^n \left(-\ln \frac{M2}{\mu^2} \right) - \frac{n+5}{2n} \right) - \theta(n-1) \left(\tilde{\psi}(n) - \frac{2}{n} \right) \right\} \quad (\text{A16})$$

$$\mathcal{B}_{M^2 I_{204(3)}} = \frac{\langle g_s^2 \bar{q}q \rangle^2}{972\pi^2 M^6} m_q \left\{ 2\delta^{0n} - 2n(-1)^n \theta(n-1) \left(\left(-\ln \frac{M2}{\mu^2} \right) - \frac{2n+3}{2n} \right) - \theta(n-2) \left(n\tilde{\psi}(n) - ((-1)^n + n) \right) \right\} \quad (\text{A17})$$

$$\mathcal{B}_{M^2 I_{220(0)}} = -\frac{\langle \alpha_s G^2 \rangle}{24\pi M^4} m_q \left[\theta(n-1)n \left(-\ln \frac{M2}{\mu^2} \right) + (-1)^n \theta(n-2) \left(n\tilde{\psi}(n) - (-1)^n - 1 \right) \right], \quad (\text{A18})$$

$$\mathcal{B}_{M^2 I_{222(1)}} = -\frac{\langle g_s^3 f G^3 \rangle}{192\pi^2 M^6} m_q \left[2\theta(n-1) \left(n \left(-\ln \frac{M2}{\mu^2} \right) - 1 \right) + n\theta(n-2)(-1)^n \tilde{\psi}(n) \right], \quad (\text{A19})$$

$$\mathcal{B}_{M^2 I_{222(2)}} = \frac{\langle g_s^3 f G^3 \rangle}{192\pi^2 M^6} m_q \left[2(-1)^n \theta(n-1) \left(n \left(-\ln \frac{M2}{\mu^2} \right) - 1 \right) + \theta(n-2) \tilde{\psi}(n) \right], \quad (\text{A20})$$

$$\mathcal{B}_{M^2 I_{240(0)}} = \frac{16 \langle g_s^2 \bar{q}q \rangle^2 + 27 \langle g_s^3 f G^3 \rangle}{5184\pi^2 M^6} m_q n \left[2\theta(n-1) \left(n \left(-\ln \frac{M2}{\mu^2} \right) - 1 \right) + (-1)^n \theta(n-2) \left(n\tilde{\psi}(n) - (-1)^n - 1 \right) \right], \quad (\text{A21})$$

$$\mathcal{B}_{M^2 I_{303(1)}} = \frac{5 \langle g_s^2 \bar{q}q \rangle^2}{486\pi^2 M^6} m_q \left[-2\delta^{0n} + (-1)^n \left(2n \left(-\ln \frac{M2}{\mu^2} \right) - n - 3 \right) + \theta(n-2) \left(n\tilde{\psi}(n) - (-1)^n n - 1 \right) \right], \quad (\text{A22})$$

$$\mathcal{B}_{M^2 I_{303(2)}} = \frac{5 \langle g_s^2 \bar{q}q \rangle^2}{972\pi^2 M^6} m_q \left\{ 8\delta^{0n} - 10\delta^{1n} + 6 \left(-\ln \frac{M2}{\mu^2} \right) - \theta(n-2) \left[3 \left(\left(-\ln \frac{M2}{\mu^2} \right) - \frac{n^2 - 7n + 3}{n(n-1)} \right) + (-1)^n \left(3(2n-1) \times \left(-\ln \frac{M2}{\mu^2} \right) - \frac{n^3 + 12n^2 - 13n + 3}{n(n-1)} \right) \right] - 3\theta(n-3) \left[\frac{1}{2} \left(2n-1 - (-1)^n \right) \tilde{\psi}(n) - \frac{1}{n-1} \left((-1)^n (n^2 - 2n) + n \right) \right] \right\}, \quad (\text{A23})$$

$$\mathcal{B}_{M^2 I_{303(3)}} = \frac{5 \langle g_s^2 \bar{q}q \rangle^2}{972\pi^2 M^6} m_q \left\{ (-1)^n \left(10\delta^{1n} - 8\delta^{0n} - 6 \left(-\ln \frac{M2}{\mu^2} \right) \right) + \theta(n-2) \left[(-1)^n \left(3 \left(-\ln \frac{M2}{\mu^2} \right) - \frac{n^2 - 7n + 3}{n(n-1)} \right) + 3(2n-1) \times \left(-\ln \frac{M2}{\mu^2} \right) - \frac{n^3 + 12n^2 - 13n + 3}{n(n-1)} \right] + 3\theta(n-3) \left[\frac{1}{2} \left((-1)^n (2n-1) - 1 \right) \tilde{\psi}(n) - \frac{1}{n-1} \left(n^2 - 2n + (-1)^n n \right) \right] \right\}, \quad (\text{A24})$$

$$\mathcal{B}_{M^2 I_{303(4)}} = \frac{5 \langle g_s^2 \bar{q}q \rangle^2}{486\pi^2 M^6} m_q \left[2\delta^{0n} - 2n\theta(n-1) \left(2n \left(-\ln \frac{M2}{\mu^2} \right) - n - 3 \right) - (-1)^n \theta(n-2) \left(n\tilde{\psi}(n) - (-1)^n n - 1 \right) \right], \quad (\text{A25})$$

$$\mathcal{B}_{M^2 I_{330(1)}} = \frac{\langle g_s^2 \bar{q}q \rangle^2}{486\pi^2 M^6} m_q \left[2\theta(n-1) \left(n \left(-\ln \frac{M2}{\mu^2} \right) - 1 \right) + (-1)^n n\theta(n-2) \tilde{\psi}(n) \right], \quad (\text{A26})$$

$$\mathcal{B}_{M^2 I_{330(2)}} = \frac{\langle g_s^2 \bar{q}q \rangle^2}{486\pi^2 M^6} m_q n \left[2\theta(n-1) \left(n \left(-\ln \frac{M2}{\mu^2} \right) - 1 \right) + (-1)^n \theta(n-2) \left(n\tilde{\psi}(n) - (-1)^n - 1 \right) \right], \quad (\text{A27})$$

$$\mathcal{B}_{M^2 I_{330(3)}} = -\frac{\langle g_s^2 \bar{q}q \rangle^2}{243\pi^2 M^6} m_q n \left[\theta(n-1) \left(4n \left(-\ln \frac{M2}{\mu^2} \right) - 5 \right) + 2(-1)^n \theta(n-2) \left(n\tilde{\psi}(n) - (-1)^n - 1 \right) \right], \quad (\text{A28})$$

$$\mathcal{B}_{M^2 I_{400(0)}} = \frac{\langle \alpha_s G^2 \rangle}{8\pi M^4} m_q \left[- (2n+1) \left(-\ln \frac{M2}{\mu^2} \right) + n + 2 - \theta(n-2) \left((-1)^n \frac{2n+1}{2} \tilde{\psi}(n) - (n+1) \frac{n+(-1)^n}{n} \right) \right], \quad (\text{A29})$$

$$\mathcal{B}_{M^2 I_{402(1)}} = \frac{(\langle 8g_s^2 \bar{q}q \rangle^2 + 81 \langle g_s^3 f G^2 \rangle) m_q}{5184\pi^2 M^6} \left\{ 2\delta^{0n} - 2n\theta(n-1) \left(\left(-\ln \frac{M2}{\mu^2} \right) - \frac{n+3}{2n} \right) - (-1)^n \theta(n-2) \left(n\tilde{\psi}(n) - ((-1)^n n + 1) \right) \right\}, \quad (\text{A30})$$

$$\mathcal{B}_{M^2 I_{402(2)}} = \frac{\langle g_s^2 \bar{q}q \rangle^2}{972\pi^2 M^6} m_q \left\{ -2\delta^{0n} + 2n\theta(n-1) \left(\left(-\ln \frac{M2}{\mu^2} \right) - \frac{2n+3}{2n} \right) + (-1)^n \theta(n-2) \left(n\tilde{\psi}(n) - ((-1)^n + n) \right) \right\}, \quad (\text{A31})$$

$$\mathcal{B}_{M^2 I_{402(3)}} = \frac{\langle g_s^2 \bar{q}q \rangle^2}{972\pi^2 M^6} m_q n \left\{ \left(2 \left(-\ln \frac{M2}{\mu^2} \right) - \frac{n+5}{2n} \right) + (-1)^n \theta(n-1) \left(\tilde{\psi}(n) - \frac{2}{n} \right) \right\}, \quad (\text{A32})$$

$$\mathcal{B}_{M^2 I_{420(1)}} = -\frac{\langle g_s^2 \bar{q}q \rangle^2 n}{648\pi^2 M^6} m_q \left[\theta(n-1) \left(\left(-\ln \frac{M2}{\mu^2} \right) - \frac{1}{n} \right) + \theta(n-2) (-1)^n \tilde{\psi}(n) \right], \quad (\text{A33})$$

$$\mathcal{B}_{M^2 I_{420(2)}} = \frac{8 \langle g_s^2 \bar{q}q \rangle^2 - 27 \langle g_s^3 f G^3 \rangle}{2592\pi^2 M^6} m_q n \left\{ \theta(n-1) \left((1-2n) \left(-\ln \frac{M2}{\mu^2} \right) + n + 3 - \frac{1}{n} \right) - \theta(n-3) \left[(-1)^n \left(\frac{2n-1}{2} \tilde{\psi}(n) - 1 \right) - n \right] \right\}, \quad (\text{A34})$$

$$\mathcal{B}_{M^2 I_{420(3)}} = \frac{\langle g_s^2 \bar{q}q \rangle^2}{486\pi^2 M^6} m_q \left[2n\delta^{1n} \left(\left(-\ln \frac{M2}{\mu^2} \right) - 2 \right) - 2n^2 \theta(n-2) \left(\left(-\ln \frac{M2}{\mu^2} \right) - 1 - \frac{1}{n} \right) + (-1)^n \theta(n-3) \left(n^2 \tilde{\psi}(n) \right. \right.$$

$$-\frac{1}{2}(-1)^n(2n^2 + 2(1 + (-1)^n) + (-1)^n - 1)\Bigg)\Bigg], \quad (\text{A35})$$

$$\mathcal{B}_{M^2} I_{420(4)} = \frac{\langle g_s^2 \bar{q}q \rangle^2}{972\pi^2 M^6} m_q \left\{ 4n(n-1)\theta(n-2) \left(\left(-\ln \frac{M^2}{\mu^2} \right) - \frac{1}{2} \right) + (-1)^n \theta(n-3) \left(2n(n-1)\tilde{\psi}(n) - ((-1)^n(4n-3) + 2n-1) \right) \right\} \quad (\text{A36})$$

$$\mathcal{B}_{M^2} I_{600(1)} = \frac{17\langle g_s^2 \bar{q}q \rangle^2}{648\pi^2 M^6} m_q \left[2\delta^{0n} - \theta(n-1)2n \left(-\ln \frac{M^2}{\mu^2} \right) + n+3 - \theta(n-2) \left((-1)^n n \tilde{\psi}(n) - 1 - (-1)^n n \right) \right], \quad (\text{A37})$$

$$\mathcal{B}_{M^2} I_{600(2)} = -\frac{88\langle g_s^2 \bar{q}q \rangle^2 - 81\langle g_s^3 fG^3 \rangle}{2592\pi^2 M^6} m_q \left\{ \frac{\delta^{0n}}{2} - 2n^2 \left(-\ln \frac{M^2}{\mu^2} \right) + \frac{7n^2 + 19n + 2}{4} - \theta(n-3)(-1)^n \left[n^2 \tilde{\psi}(n) - \frac{1}{4} \left(5n^2 + n + (-1)^n(4n+2) \right) \right] \right\}, \quad (\text{A38})$$

-
- [1] R. Ammar, R. Davis, W. Kropac, J. Mott, D. Slate, B. Werner, M. Derrick, T. Fields and F. Schweingruber, Bosen resonance of mass 980 MeV decaying into $\pi^- \eta$, *Phys. Rev. Lett.* **21**, 1832-1835 (1968).
- [2] R. L. Jaffe, Multi-quark hadrons. 1. The phenomenology of (2 quark 2 anti-quark) mesons, *Phys. Rev. D* **15**, 267 (1977).
- [3] M. G. Alford and R. L. Jaffe, Insight into the scalar mesons from a lattice calculation, *Nucl. Phys. B* **578**, 367-382 (2000). [[hep-lat/0001023](#)]
- [4] T. Humanic [ALICE Collaboration], Studying the $a_0(980)$ tetraquark candidate using $K_s^0 K^\pm$ interactions in the LHC ALICE collaboration, *Rev. Mex. Fis. Suppl.* **3**, 0308039(2022) .
- [5] T. V. Brito, F. S. Navarra, M. Nielsen and M. E. Bracco, QCD sum rule approach for the light scalar mesons as four-quark states, *Phys. Lett. B* **608**, 69-76 (2005). [[hep-ph/0411233](#)]
- [6] E. Klempt and A. Zaitsev, Glueballs, hybrids, multi-quarks. Experimental facts versus QCD inspired concepts, *Phys. Rept.* **454** 1-202 (2007). [[arXiv:0708.4016](#)]
- [7] J. D. Weinstein and N. Isgur, Do Multi-Quark Hadrons Exist?, *Phys. Rev. Lett.* **48**, 659 (1982).
- [8] T. Branz, T. Gutsche and V. E. Lyubovitskij, $f_0(980)$ -meson as a $K\bar{K}$ molecule in a phenomenological Lagrangian approach, *Eur. Phys. J. A* **37**, 303 (2008). [[arXiv:0712.0354](#)]
- [9] L. Y. Dai, X. G. Wang and H. Q. Zheng, Pole Analysis of Unitarized One Loop χ PT Amplitudes - A Triple Channel Study, *Commun. Theor. Phys.* **58**, 410-414 (2012). [[arXiv:1206.5481](#)]
- [10] L. Y. Dai and M. R. Pennington, Two photon couplings of the lightest isoscalars from BELLE data, *Phys. Lett. B* **736**, 11-15 (2014). [[arXiv:1403.7514](#)]
- [11] T. Sekihara and S. Kumano, Constraint on $K\bar{K}$ compositeness of the $a_0(980)$ and $f_0(980)$ resonances from their mixing intensity, *Phys. Rev. D* **92**, 034010 (2015). [[arXiv:1409.2213](#)]
- [12] M. Ablikim *et al.* [BESIII Collaboration], Observation of the semileptonic decay $D^0 \rightarrow a_0(980)^- e^+ \nu_e$ and evidence for $D^+ \rightarrow a_0(980)^0 e^+ \nu_e$, *Phys. Rev. Lett.* **121**, 081802 (2018). [[arxiv:1803.02166](#)]
- [13] M. Ablikim *et al.* [BESIII Collaboration], Study of light scalar mesons through $D_s^+ \rightarrow \pi^0 \pi^0 e^+ \nu_e$ and $K_S^0 K_S^0 e^+ \nu_e$ decays, *Phys. Rev. D* **105**, L031101 (2022).
- [14] N. R. Soni, A. N. Galaria, J. J. Patel and J. N. Pandya, Semileptonic decays of charmed mesons to light scalar mesons, *Phys. Rev. D* **102**, 016013 (2020). [[arXiv:2001.10195](#)]
- [15] X. D. Cheng, H. B. Li, B. Wei, Y. G. Xu and M. Z. Yang, Study of $D \rightarrow a_0(980) e^+ \nu_e$ decay in the light-cone sum rules approach, *Phys. Rev. D* **96**, 033002 (2017). [[arXiv:1706.01019](#)]
- [16] Q. Huang, Y. J. Sun, D. Gao, G. H. Zhao, B. Wang and W. Hong, Study of form factors and branching ratios for $D \rightarrow S, Al \bar{l}$ with light-cone sum rules, [[arXiv:2102.12241](#)]
- [17] S. Momeni and M. Saghebfar, Semileptonic D -meson decays to the vector, axial vector and scalar mesons in Hard-Wall AdS/QCD correspondence, *Eur. Phys. J. C* **82**, 473 (2022).
- [18] H. Y. Cheng, C. K. Chua and K. C. Yang, Charmless hadronic B decays involving scalar mesons: Implications to the nature of light scalar mesons, *Phys. Rev. D* **73**, 014017 (2006). [[hep-ph/0508104](#)]
- [19] V. A. Novikov, M. A. Shifman, A. I. Vainshtein and V. I. Zakharov, Calculations in external fields in quantum chromodynamics. Technical review, *Fortsch. Phys.* **32**, 585 (1984).
- [20] W. Hubschmid and S. Mallik, Operator expansion at short distance in QCD, *Nucl. Phys. B* **207**, 29-42 (1982).
- [21] J. Govaerts, F. de Viron, D. Gusbin and J. Weyers, Exotic mesons from QCD sum rules, *Phys. Lett. B* **128**, 262 (1983).
- [22] J. Govaerts, F. de Viron, D. Gusbin and J. Weyers, QCD sum rules and hybrid mesons, *Nucl. Phys. B* **248**, 1-18 (1984).
- [23] J. Ambjorn and R. J. Hughes, Canonical quantization in nonabelian background fields. 1., *Annals Phys.* **145**, 340 (1983).
- [24] J. Ambjorn and R. J. Hughes, Gauge fields, BRS symmetry and the sasimir effect, *Nucl. Phys. B* **217**, 336-348 (1983).
- [25] L. J. Reinders, H. Rubinstein and S. Yazaki, Hadron properties from QCD sum rules, *Phys. Rept.* **127**, 1 (1985).

- [26] V. Elias, T. G. Steele and M. D. Scadron, $q\bar{q}$ and higher dimensional condensate contributions to the nonperturbative quark mass, *Phys. Rev. D* **38**, 1584 (1988).
- [27] T. Huang, X. N. Wang, X. d. Xiang and S. J. Brodsky, The quark mass and spin effects in the mesonic structure, *Phys. Rev. D* **35**, 1013 (1987).
- [28] T. Huang and Z. Huang, Quantum chromodynamics in background fields, *Phys. Rev. D* **39** 1213 (1989).
- [29] H. B. Fu, X. G. Wu, W. Cheng and T. Zhong, ρ meson longitudinal leading-twist distribution amplitude within QCD background field theory, *Phys. Rev. D* **94**, no.7, 074004 (2016). [arXiv:1607.04937]
- [30] D. D. Hu, H. B. Fu, T. Zhong, L. Zeng, W. Cheng and X. G. Wu, $\eta^{(\prime)}$ meson twist-2 distribution amplitude within QCD sum rule approach and its application to the semi-leptonic decay $D_s^+ \rightarrow \eta^{(\prime)} \ell^+ \nu_\ell$, *Eur. Phys. J. C* **82**, 12 (2022). [arXiv:2102.05293]
- [31] D. D. Hu, H. B. Fu, T. Zhong, Z. H. Wu and X. G. Wu, $a_1(1260)$ meson longitudinal twist-2 distribution amplitude and the $D \rightarrow a_1(1260) \ell^+ \nu_\ell$ decay processes, *Eur. Phys. J. C* **82**, 603 (2022). [arXiv:2107.02758]
- [32] T. Zhong, X. G. Wu, Z. G. Wang, T. Huang, H. B. Fu and H. Y. Han, Revisiting the pion leading-twist distribution amplitude within the QCD background field theory, *Phys. Rev. D* **90**, 016004 (2014) [arXiv:1405.0774]
- [33] H. B. Fu, L. Zeng, W. Cheng, X. G. Wu and T. Zhong, Longitudinal leading-twist distribution amplitude of the J/ψ meson within the background field theory, *Phys. Rev. D* **97**, 074025 (2018). [arXiv:1801.06832]
- [34] T. Zhong, X. G. Wu, T. Huang and H. B. Fu, Heavy pseudoscalar twist-3 distribution amplitudes within QCD theory in background fields, *Eur. Phys. J. C* **76**, 509 (2016). [arXiv:1604.04709]
- [35] T. Huang, X. H. Wu and M. Z. Zhou, Twist three distribute amplitudes of the pion in QCD sum rules, *Phys. Rev. D* **70**, 014013 (2004). [hep-ph/0402100]
- [36] T. Zhong, X. G. Wu, H. Y. Han, Q. L. Liao, H. B. Fu and Z. Y. Fang, Revisiting the twist-3 distribution amplitudes of K meson within the QCD background field approach, *Commun. Theor. Phys.* **58**, 261-270 (2012). [arXiv:1109.3127]
- [37] T. Zhong, Z. H. Zhu and H. B. Fu, Constraint of ξ -moments calculated with QCD sum rules on the pion distribution amplitude models, arXiv:2209.02493.
- [38] T. Zhong, Z. H. Zhu, H. B. Fu, X. G. Wu and T. Huang, Improved light-cone harmonic oscillator model for the pionic leading-twist distribution amplitude, *Phys. Rev. D* **104**, 016021 (2021). [arXiv:2102.03989]
- [39] T. Zhong, H. B. Fu and X. G. Wu, Investigating the ratio of CKM matrix elements $|V_{ub}|/|V_{cb}|$ from semileptonic decay $B_s^0 \rightarrow K^- \mu^+ \nu_\mu$ and kaon twist-2 distribution amplitude, *Phys. Rev. D* **105**, 116020 (2022). [arXiv:2201.10820]
- [40] X. G. Wu and T. Huang, An implication on the pion distribution amplitude from the pion-photon transition form factor with the new BaBar data, *Phys. Rev. D* **82** 034024 (2010). [arXiv:1005.3359]
- [41] X. G. Wu and T. Huang, Constraints on the light pseudoscalar meson distribution amplitudes from their meson-photon transition form factors, *Phys. Rev. D* **84** 074011 (2011). [arXiv:1106.4365]
- [42] T. Huang, B. Q. Ma and Q. X. Shen, Analysis of the pion wave function in light cone formalism, *Phys. Rev. D* **49** 1490 (1994). [hep-ph/9402285]
- [43] F. G. Cao and T. Huang, Large corrections to asymptotic $F(\eta_c \gamma)$ and $F(\eta_b \gamma)$ in the light cone perturbative QCD, *Phys. Rev. D* **59** 093004 (1999). [hep-ph/9711284]
- [44] T. Huang and X. G. Wu, A Model for the twist-3 wave function of the pion and its contribution to the pion form-factor, *Phys. Rev. D* **70** 093013 (2004). [hep-ph/0408252]
- [45] X. G. Wu and T. Huang, Pion electromagnetic form-factor in the $K_{(T)}$ factorization formulae, *Int. J. Mod. Phys. A* **21** 901(2006). [hep-ph/0507136]
- [46] T. Zhong, Y. Zhang, X. G. Wu, H. B. Fu and T. Huang, The ratio $\mathcal{R}(D)$ and the D -meson distribution amplitude, *Eur. Phys. J. C* **78** 937 (2018). [arXiv:1807.03453]
- [47] T. Huang, X. G. Wu and T. Zhong, Finding a way to determine the pion distribution amplitude from the experimental data, *Chin. Phys. Lett.* **30**, 041201 (2013). [arXiv:1303.2301]
- [48] T. Huang, T. Zhong and X. G. Wu, Determination of the pion distribution amplitude, *Phys. Rev. D* **88**, 034013 (2013). [arXiv:1305.7391]
- [49] X. G. Wu, T. Huang and T. Zhong, Information on the pion distribution amplitude from the pion-photon transition form factor with the Belle and BaBar data, *Chin. Phys. C* **37**, 063105 (2013). [arXiv:1206.0466]
- [50] T. Zhong, X. G. Wu and T. Huang, The longitudinal and transverse distributions of the pion wave function from the present experimental data on the pion-photon transition form factor, *Eur. Phys. J. C* **76**, 390 (2016). [arXiv:1510.06924]
- [51] Y. Zhang, T. Zhong, H. B. Fu, W. Cheng and X. G. Wu, D_s meson leading-twist distribution amplitude within the QCD sum rules and its application to the $B_s \rightarrow D_s$ transition form factor, *Phys. Rev. D* **103**, 114024 (2021). [arXiv:2104.00180]
- [52] H. Y. Han, X. G. Wu, H. B. Fu, Q. L. Zhang and T. Zhong, Twist-3 distribution amplitudes of scalar mesons within the QCD sum rules and its application to the $B \rightarrow S$ transition form factors, *Eur. Phys. J. A* **49**, 78 (2013). [arXiv:1301.3978]
- [53] C. D. Lü, Y. M. Wang and H. Zou, Twist-3 distribution amplitudes of scalar mesons from QCD sum rules, *Phys. Rev. D* **75**, 056001 (2007). [hep-ph/0612210]
- [54] S. Narison, Improved $f_{D_{(s)}^*}$, $f_{B_{(s)}^*}$ and f_{B_c} from QCD Laplace sum rules, *Int. J. Mod. Phys. A* **30** 1550116(2015). [arXiv:1404.6642]
- [55] P. Colangelo and A. Khodjamirian, QCD sum rules, a modern perspective, [hep-ph/0010175]
- [56] K. C. Yang, W. Y. P. Hwang, E. M. Henley and L. S. Kisslinger, QCD sum rules and neutron proton mass difference, *Phys. Rev. D* **47** 3001-3012 (1993).
- [57] W. Y. P. Hwang and K. C. Yang, QCD sum rules: $\Delta - N$ and $\Sigma^0 - \Lambda$ mass splittings, *Phys. Rev. D* **49** 460(1994).
- [58] P. A. Zyla *et al.* [Particle Data Group], Review of particle physics, *Prog. Theor. Exp. Phys.* **2020** 083C01(2020).
- [59] T. Huang and Z. H. Li, The binding energy of the excited heavy light mesons in HQET, *Phys. Lett. B* **438**, 159-164 (1998).
- [60] Z. H. Li, N. Zhu, X. J. Fan and T. Huang, Form factors $f_+^{B \rightarrow \pi}(0)$ and $f_+^{D \rightarrow \pi}(0)$ in QCD and determination of $|V_{ub}|$ and $|V_{cd}|$, *JHEP* **05**, 160 (2012). [arxiv:1206.0091]

- [61] A. Bharucha, D. M. Straub and R. Zwicky, $B \rightarrow V\ell^+\ell^-$ in the standard model from light-cone sum rules, *JHEP* **08**, 098 (2016). [[arxiv:1503.05534](#)]
- [62] C. Bourrely, I. Caprini and L. Lellouch, Model-independent description of $B \rightarrow \pi\ell\nu$ decays and a determination of $|V_{ub}|$, *Phys. Rev. D* **79**, 013008 (2009). [[arxiv:0807.2722](#)]
- Phys.Rev.D79:013008,2009
- [63] H. B. Fu, L. Zeng, R. Lü, W. Cheng and X. G. Wu, The $D \rightarrow \rho$ semileptonic and radiative decays within the light-cone sum rules, *Eur. Phys. J. C* **80**, 194 (2020). [[arXiv:1808.06412](#)]